E-ISSN 2667-4610

bulletin of UROONCOLOGY

galenos yayinevi

UROONCOLOGY ASSOCIATION - 1999

March 2026

Volume 25(1)

The Official Journal of Urooncology Association of Turkey

Editorial Board

Please refer to the journal's webpage https://uroonkolojibulteni.com/) for "Journal Policies", "Instructions to Authors" and "Aims and Scope".

The Bulletin of Urooncology is included in leading international databases. Currently, the Bulletin of Urooncology is indexed in **Emerging Sources Citation Index (ESCI), DOAJ (Directory of Open Access Journals), TUBITAK/ULAKBIM Turkish Medical Database, EBSCO, Embase, CINAHL Complete Database, Gale/Cengage Learning, ProQuest, J-Gate, Turk Medline, Hinari, GOALI, ARDI, OARE, AGORA, CNKI** and **Turkiye Citation Index**.

The journal is published on Internet.

Owner: Güven Aslan on Behalf of Turkish Urooncology Association

Responsible Manager: Bahadır Şahin

Reviewing the articles' conformity to the publishing standards of the Journal, typesetting, reviewing and editing the manuscripts and abstracts in English, creating links to source data, and publishing process are realized by Galenos.

Publisher Contact
Address: Molla Gürani Mah. Kaçamak Sk. No: 21/1
34093 İstanbul, Türkiye
Phone: +90 (530) 177 30 97
E-mail: info@galenos.com.tr/yayin@galenos.com.tr
Web: www.galenos.com.tr
Publisher Certificate Number: 14521

Online Publication Date: March 2026
E-ISSN: 2667-4610
International scientific journal published quarterly.

Contents

Original Articles

Case Report

bulletin of
UROONCOLOGY

BEST REVIEWER of ISSUE
Çağrı Akın ŞEKERCİ

Original Article

DOI: 10.4274/uob.galenos.2025.2025.8.4

Bull Urooncol 2026;25(1):1-6

Prostate-specific Antigen Density and Clinically Significant Prostate Cancer: Impact of Prostatic Volume in PI-RADS 3 Lesions; High Volume Single-center Analysis

Çağrı Akpınar[1], Diğdem Kuru Öz[2], Ahmet Furkan Özsoy[1], Eriz Özden[2], Nuray Haliloğlu[2], Araz Musayev[1], Serhat Erkmen[1], Muhammed Arif İbiş[1], Murat Can Karaburun[3], Çağatay Göğüş[1], Evren Süer[1], Sümer Baltacı[1]

[1]*Ankara University Faculty of Medicine, Department of Urology, Ankara, Türkiye*
[2]*Ankara University Faculty of Medicine, Department of Radiology, Ankara, Türkiye*
[3]*University of Health Sciences Türkiye, Ankara Etlik City Hospital, Department of Urology, Ankara, Türkiye*

Abstract

Objective: Prostate-specific antigen density (PSAd) has gained traction as a superior diagnostic marker, compared with PSA alone, for predicting clinically significant prostate cancer (csPCa). However, prostate gland volume may affect the diagnostic accuracy of PSAd. To evaluate how prostate volume influences the diagnostic performance of PSAd for detecting csPCa in patients with Prostate Imaging Reporting and Data System (PI-RADS) 3 lesions.

Materials and Methods: We retrospectively analyzed 576 patients with PI-RADS 3 lesions who underwent PSA testing, multiparametric magnetic resonance imaging (MRI), and cognitive- and fusion-guided transrectal prostate biopsies between 2017 and 2025. PSAd was calculated as serum PSA divided by MRI-measured prostate volume. Patients were stratified into three groups according to prostate volume: ≤30 mL, 31-50 mL, and ≥51 mL. csPCa was defined as International Society of Urological Pathology grade ≥2. Diagnostic performance of PSAd was assessed using receiver operating characteristic (ROC) curve analysis with volume-specific cut-offs.

Results: The overall csPCa detection rate was significantly higher in patients with prostates ≤30 mL ($p<0.001$). Across all volume groups, csPCa detection remained <5% when PSAd <0.10 ng/mL/mL. For glands ≤30 mL, csPCa rates rose sharply above this threshold. ROC analysis revealed that small prostates had a slightly higher diagnostic accuracy [area under the curve (AUC) 0.668] compared with intermediate (AUC 0.599) and large (AUC 0.633) glands. Optimal PSAd cut-offs were narrowly distributed (0.1058-0.1531), but diagnostic sensitivity varied with volume.

Conclusion: The findings indicate that the diagnostic performance of PSAd in predicting csPCa is influenced by prostate volume. Instead of proposing definitive universal cut-off values, our results suggest that lower PSAd thresholds may be considered in patients with larger prostate volumes, particularly in borderline cases such as PI-RADS 3 lesions. Incorporating prostate volume into PSAd interpretation may improve risk stratification and contribute to more individualized biopsy decision-making.

Keywords: Multiparametric magnetic resonance imaging, PI-RADS, prostate cancer, PSA density, PSMA

Introduction

Prostate cancer (PCa) remains one of the most prevalent malignancies affecting men globally, with significant implications for both morbidity and mortality. Current diagnostic pathways often begin with serum prostate-specific antigen (PSA) testing and digital rectal examination, followed by multiparametric magnetic resonance imaging (mpMRI) and biopsy when indicated (1,2). Despite its utility, serum PSA is influenced by various benign conditions, particularly benign prostatic hyperplasia, thereby reducing its specificity for detecting clinically significant PCa (csPCa).

To overcome this limitation, PSA density (PSAd), defined as the ratio of serum PSA to prostate volume, has been proposed as a

Cite this article as: Akpınar Ç, Kuru Öz D, Özsoy AF, et al. Prostate-specific antigen density and clinically significant prostate cancer: impact of prostatic volume in PI-RADS 3 lesions; high volume single-center analysis. Bull Urooncol. 2026;25(1):1-6.

Address for Correspondence: Ahmet Furkan Özsoy, MD, Ankara University Faculty of Medicine, Department of Urology, Ankara, Türkiye
E-mail: furkanozsoy22@gmail.com **ORCID:** orcid.org/0000-0001-8134-7484
Received: 15.08.2025 **Accepted:** 26.11.2025 **Publication Date:** 18.03.2026

more refined marker for csPCa. PSAd has demonstrated higher predictive value for csPCa compared to PSA alone, particularly in cases where MRI findings are equivocal, such as Prostate Imaging Reporting and Data System (PI-RADS) 3 lesions (3-6). Guidelines such as those from the European Association of Urology (EAU) and National Institute for Health and Care Excellence recently suggest the integration of PSAd into clinical decision-making, especially for PI-RADS 3 lesions (7).

PSAd is used to aid decision-making in cases of indeterminate PI-RADS 3 lesions on MRI. In patients with PI-RADS 3 lesions and a PSAd below 0.10 ng/mL/mL, biopsy may be deferred due to the low risk of csPCa (4,8), whereas biopsy is recommended when PSAd is 0.10 ng/mL/mL or higher (7). However, the use of fixed PSAd thresholds may not account for differences in prostate size. Larger prostates typically produce higher PSA levels because of increased benign prostatic tissue, thereby potentially obscuring the contribution of malignant foci. Conversely, smaller glands may yield elevated PSAd values for relatively insignificant cancers. Despite its increasing use in biopsy decision-making, there are limited studies investigating how prostate volume alters the diagnostic performance of PSAd (9).

This study aims to evaluate, within a high-volume, single-center cohort of 576 PI-RADS 3 lesions, the influence of prostate volume on PSAd for detecting csPCa. In our study, by examining PSAd thresholds across stratified prostate volume groups, we hope to determine whether volume-adjusted interpretations could improve diagnostic accuracy and more effectively guide biopsy strategies.

Materials and Methods

Patients and Methods

This retrospective study was conducted in 576 patients with PI-RADS 3 lesions who underwent transrectal ultrasonography (TRUS)-guided biopsies for suspected PCa at our tertiary institution between January 2017 and January 2025. Written informed consent was obtained from all patients before TRUS-guided biopsies. All procedures were performed in accordance with the 1964 Declaration of Helsinki and its later amendments. The study was approved by our Institutional Ethics Committee of Ankara University (decision no: İ06-596-25, date: 12.08.2025).

All patients were biopsy-naive and had a clinical suspicion of PCa based on either elevated PSA levels or abnormal findings on digital rectal examination. After serum PSA testing, mpMRI, and transrectal ultrasound-guided cognitive (E.Ö.) and fusion-targeted prostate biopsy (N.H.) within the diagnostic pathway. Patients presenting with PSA levels above 40 ng/mL were excluded because these levels are commonly associated with advanced or metastatic PCa and may bias the analysis of localized disease.

All patients were scanned on a 3T MRI scanner within three months before the biopsy. For image assessment, all mpMRI examinations performed before 2019 were re-reviewed by an experienced abdominal radiologist (D.K.Ö., with 10 years of expertise in prostate MRI) according to the PI-RADS v2.1 criteria. All PI-RADS 3 lesions identified after 2019 were reassessed. Total prostate volume was calculated on MRI using the ellipsoid formula (10), and divided into three groups according to volumes ≤30 mL, 31-50 mL, and ≥51 mL biopsy specimens were evaluated according to the International Society of Urological Pathology (ISUP) modified Gleason system (11). csPCa is defined on histopathology as a Gleason score ≥ 3+4 (≥ISUP grade 2), per-lesion basis. PSAd was calculated as PSA divided by prostate volume. Diagnostic performance was analyzed at thresholds of <0.10, 0.10-0.14, 0.15-0.19 and ≥0.20 ng/mL/mL

MR Image Acquisition Technique

mpMRI images were obtained using a 3.0 Tesla MR system (Verio; Siemens Medical Solutions, Erlangen, Germany). A standard body-matrix coil was used to receive signals from the patients' prostates. The MRI scanning procedure incorporated three-directional (3D) (sagittal, coronal, and axial) T2 turbo spin-echo (TSE) imaging; axial diffusion-weighted imaging sequences performed at three b-values (0, 1000, and 2000 mm^2/s) using echo-planar technology; and an axial TSE T2-weighted sequence encompassing pelvic lymph nodes to the level of the aortic bifurcation. After injecting gadolinium contrast medium (0.2 mL/kg) into the vein at 2.5 mL/s, followed by 15 mL of saline, dynamic contrast-enhanced images were obtained in the axial plane using a fat-suppressed 3D T1 VIBE protocol.

TRUS Biopsy Procedure

TRUS was using GE P5 or LOGIQ S8 ultrasound scanners (GE Healthcare, Milwaukee, Wisconsin) equipped with a biplanar convex/convex transrectal probe (BE9CS). The biopsies were performed via the transrectal route using a fully automatic core biopsy device with an 18-gauge, 25 cm tru-cut needle (Geotek). The T2W axial images were loaded onto the ultrasound machine, and after fusing selected images with real-time TRUS images, a fusion biopsy was performed with at least three samples taken from the target lesion (N.H). Subsequently, a 12-core systematic biopsy was performed. Prior to cognitive biopsy, the locations of suspicious lesions were reviewed by the operator (E.Ö.), and three additional cores from the region of the index lesion were taken using cognitive TRUS guidance. All biopsy procedures were performed by the two operators, each with more than 10 years of experience in TRUS-guided prostate biopsy. All biopsy specimens were labelled according to the site of the prostate that was biopsied and were sent for histopathologic evaluation.

Statistical Analysis

Statistical analyses were performed using SPSS® Statistics version 26.0 (IBM Corp., Armonk, NY, USA). Patient characteristics were reported using descriptive statistics. Descriptive statistics were expressed as medians and interquartile ranges for variables that were not normally distributed. The chi-square and Fisher's exact tests were used to compare categorical variables between groups. The diagnostic performance of PSAd was assessed across prostate volume groups using the area under the receiver operating characteristic (ROC) curve (AUC). Optimal cut-off points were determined such that sensitivity and specificity were balanced. A p-value of less than 0.05 at the 95% confidence level was considered to indicate statistical significance.

Results

The cohort consisted of 576 patients. Patient characteristics for those with PI-RADS 3 lesions who underwent biopsy are shown in Table 1. The median age was 64 years, the median PSA was 6.5 ng/mL, and the median PSAd was 0.11 ng/mL/mL. The median prostate volume was 65 mL, and the maximum prostate volume was 255 mL. Among all patients with PI-RADS 3 lesions, those with a prostate volume ≤30 mL had a significantly higher rate of csPCa compared to those with volumes of 31-50 mL and ≥51 mL (p<0.001).

For PSAd values below 0.10 ng/mL/mL, the rate of csPCa remained under 5% across all prostate volume groups. Among patients with prostate volumes ≤30 mL, csPCa rates were consistently higher at all PSAd levels above 0.10 ng/mL/mL compared to other volume groups, with a statistically significant difference observed in the 0.10-0.14 ng/mL/mL range (p=0.009) (Table 2). Among patients with prostate volume ≤30 mL, no csPCa was detected when PSAd was <0.10 ng/mL/mL, while detection rates were 30.8% for 0.10-0.14, 27.3% for 0.15-0.19, and 44.3% for ≥0.20 ng/mL/mL. For those with prostate volume of 31-50 mL, the corresponding rates were 4.9%, 8.3%, 11.8%, and 17.4%, while in patients with prostate volume ≥51 mL, the rates were 3.3%, 5.7%, 4%, and 17.6%, respectively (Table 2).

PSAd showed varying diagnostic accuracy across prostate volume groups. In glands ≤30 mL, the AUC was 0.668 with an optimal cut-off of 0.1441 ng/mL/mL. For prostates measuring 31-50 mL, the AUC was 0.599 and the cut-off was 0.1531 ng/mL/mL. In glands ≥51 mL, diagnostic performance remained moderate with an AUC of 0.633 and a lower optimal cut-off of 0.1058 ng/mL/mL (Table 3) (Figure 1).

Table 1. Demographic and clinical characteristics of patients with PI-RADS 3 lesions who underwent biopsy

Parameters	Overall cohort (n=576)
Age, median (IQR)	64 (59-70)
PSA (ng/mL), median (IQR)	6.5 (4.87-8.6)
Prostate MRI volume (mL) median (IQR)	65 (50-88)
PSA density (ng/mL²), median (IQR)	0.11 (0.07-0.13)
PSA density, n (%) <0.10 0.10-0.14 0.15-0.19 ≥0.20	 258 (44.8%) 190 (33.1%) 70 (12.1%) 58 (10.1%)
Biopsy procedure, Cognitive-targeted (n=223) Fusion-targeted (n=353)	 223 (38.7%) 353 (61.3%)
Biopsy results, n (%) Benign ISUP grade 1 ISUP grade ≥2	 455 (79%) 73 (12.7%) 48 (8.3%)

PSA: Prostate-specific antigen, MRI: Magnetic resonance imaging, PI-RADS: Prostate Imaging Reporting and Data System, ISUP: International Society of Urological Pathology, IQR: Interquartile range

Table 2. Clinically significant prostate cancer detection rates by PI-RADS score, PSA density and prostate volume undergoing prostate biopsy

Parameters (n=576)	Prostate volume			P-value*
	≤30 mL (n=46;8%)	31-50 mL (n=170;29.5%)	≥51 mL (n=360; 62.5%)	
csPCa detection rates				
PI-RADS 3 overall, (n=576)	15/46 (32.6%)	16/170 (9.4%)	17/360 (4.7%)	<0.001
PSA density <0.10 (n=258) PSA density 0.10-0.14 (n=190) PSA density 0.15-0.19 (n=70) PSA density ≥0.20 (n=58)	-/4 (-) 4/13 (30.8%) 3/11 (27.3%) 8/18 (44.3%)	2/41 (4.9%) 6/72 (8.3%) 4/34 (11.8%) 4/23 (17.4%)	7/213 (3.3%) 6/105 (5.7%) 1/25 (4%) 3/17 (17.6%)	0.816 0.009 0.129 0.106

*: Chi-square and Fisher's exact tests, PI-RADS: Prostate Imaging Reporting and Data System, PSA: Prostate-specific antigen, csPCa: Clinically significant prostate cancer

Table 3. Diagnostic accuracy of PSA density: AUC values and optimal cut-off points by prostate volume group

Prostate volume	AUC	%95 CI	Optimal PSAd cut-off (ng/mL/mL)
≤30 mL	0.668	0.504-0.831	0.1441
31-50 mL	0.599	0.440-0.757	0.1531
≥51 mL	0.633	0.497-0.769	0.1058

PSA: Prostate-specific antigen, AUC: Area under the curve, PSAd: PSA density, CI: Confidence interval

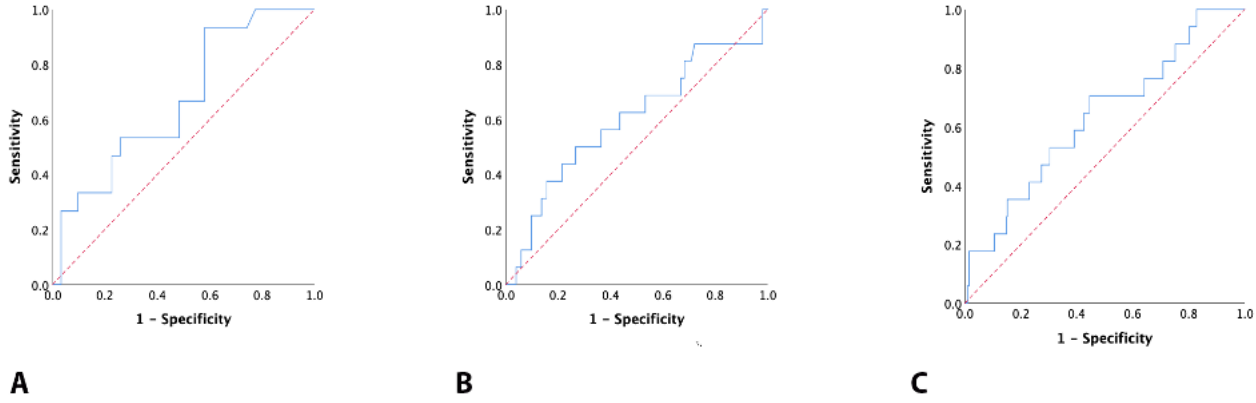

Figure 1. Receiver operating characteristic curves demonstrating the diagnostic performance of prostate-specific antigen (PSA) density for clinically significant prostate cancer across three prostate volume groups: **(A)** ≤30 mL, **(B)** 31-50 mL, and **(C)** ≥51 mL. Area under the curve values and optimal cut-off points were calculated separately for each group. The discriminative ability of PSA density varied by gland size, highlighting volume-dependent thresholds

Discussion

MRI alone has inherent limitations due to variability in interpretation among readers and between centers (1,12,13). This limitation becomes particularly critical for PI-RADS 3 "gray zone" lesions, where reported rates of csPCa diagnosis range widely from 3% to 50% (14,15). Such a broad range reflects the heterogeneity of biopsy outcomes within this lesion category, underscoring the challenge in clinical decision-making for PI-RADS 3 findings. Since PSAd is calculated using MRI and PSA values, both routinely obtained in the diagnostic workup for suspected PCa, it provides a straightforward, cost-effective metric that has been widely adopted in clinical settings. Much research has focused on identifying optimal PSAd thresholds to enhance sensitivity among patients with negative MRI findings or to improve specificity when MRI results are equivocal. Tools such as the risk-adapted biopsy decision model proposed by Schoots and Padhani (4) exemplify this approach. Furthermore, regardless of prostate volume stratification, PSAd has been demonstrated to outperform PSA alone as a predictor of csPCa (5,16).

According to the 2025 EAU guidelines, a risk-adapted strategy based on PSAd is proposed to guide biopsy decisions for PI-RADS-detected lesions. In this framework, a csPCa detection rate of <5% is considered very low risk, 5-10% is considered low risk, and 10-20% is considered intermediate risk. The minimum csPCa risk threshold for recommending biopsy is set at ≥10%. For PI-RADS 3 lesions, this risk corresponds to a PSAd of ≥0.10 ng/mL/mL, with biopsy strongly recommended at PSAd ≥0.20 ng/mL/mL. Consistent with earlier reports, Koparal et al. (17) demonstrated that a PSAd value greater than 0.20 ng/mL/mL serves as an independent predictor of csPCa in patients with PI-RADS 3 lesions. In our cohort, which included a substantial number of PI-RADS 3 lesions biopsied by two experienced operators, csPCa detection rates remained below 5% across all prostate volume groups when PSAd was <0.10, confirming the very low-risk category defined by the EAU. These findings support omitting biopsy for PI-RADS 3 lesions with PSAd <0.10, regardless of prostate size.

Univariate analysis showed that starting from a PSAd threshold of 0.10 ng/mL/mL, csPCa detection rates increased across all prostate volume groups, with the most pronounced rise observed in prostates ≤30 mL. ROC curve analysis also supported this volume-dependent diagnostic variability. While csPCa detection rates increased with rising PSAd across all prostate volume groups, ROC analysis revealed that the discriminatory power of PSAd was not uniform. Despite relatively similar optimal cut-off values, the AUC was highest in the ≤30 mL group, indicating superior diagnostic performance in small prostates. In contrast, PSAd had a lower AUC in intermediate and large prostates, suggesting reduced discriminative accuracy in these groups. Although the AUC was lower in large prostate groups (≥50 mL), setting a lower PSAd cut-off value may be beneficial for detecting csPCa in this group.

These findings suggest that applying a uniform PSAd threshold may lead to underdiagnosis of csPCa in men with large prostate volumes and unnecessary biopsies in those with small volumes. While some studies have proposed lower PSAd thresholds for large prostates to preserve sensitivity, our results support this approach. Additionally, the ability to detect csPCa at lower PSAd levels in small prostates suggests that PSAd is a more sensitive biomarker in this subgroup. Although PSAd was associated with increasing csPCa risk across all volume categories, its discriminatory power appeared to be stronger in smaller glands. Therefore, adapting PSAd thresholds according to prostate volume may improve the accuracy of clinical decision-making.

A study that evaluated PSAd in detail found that among patients with PSAd between 0.09 and 0.19 ng/mL/mL, those with a prostate volume of less than 33 mL had higher detection rates of csPCa (5). In a recent publication, Robinson et al. (18) assessed how PSAd cut-off values might vary according to prostate volume when sensitivity is held constant. They identified cut-off values of 0.21 ng/mL/mL for small prostates and 0.11 ng/mL/mL for large prostates. However, they reported that smaller prostate volumes were associated with higher sensitivity in detecting csPCa. They emphasized that these cut-off values were not intended as direct clinical recommendations, but rather to

illustrate the extent to which PSAd thresholds may need to be adjusted based on prostate volume.

Our study confirms that the diagnostic performance of PSAd in PI-RADS 3 lesions is affected by prostate size. Larger glands may dilute the PSA contribution from cancer, reducing PSAd sensitivity. However, the optimal PSAd cut-off values we identified ranged narrowly from 0.10 to 0.15 ng/mL/mL across volume groups; csPCa detection rates were notably higher in patients with smaller prostates, even at similar PSAd levels. This highlights the potential for enhanced diagnostic sensitivity in small prostate volumes and suggests that using a uniform PSAd threshold may not be equally effective for all prostate sizes. Moreover, the clinical relevance of prostate volume extends beyond this specific context. In some situations, such as when patients present with a PSAd value below 0.10 ng/mL/mL and PI-RADS 1-2 findings on mpMRI, a prostate biopsy is usually not recommended. Determining whether repeat biopsy should be performed in patients with initially negative biopsy results but persistently suspicious PI-RADS scores remains challenging in clinical practice. To enhance diagnostic precision and reduce the risk of overlooking csPCa, several complementary parameters have been explored. For example, Şahin et al. (19) reported that lesion density defined as the length of the mpMRI-detected lesion adjusted for prostate volume served as an independent predictor of csPCa. These findings highlight that prostate volume meaningfully influences both lesion density and PSAd (19).

Study Limitations

This study has several limitations. First, the retrospective design represents the main limitation and may have introduced selection bias regarding which patients with PI-RADS 3 lesions proceeded to biopsy. Another important consideration is the timing of mpMRI in relation to prostate biopsy. During the early phase of the study period (2017-2019), mpMRI was not routinely performed before the initial biopsy; therefore, biopsy-naive patients who underwent mpMRI during that interval were also included in the analysis. At our institution, however, mpMRI was already being used prior to the first biopsy in selected patients presenting with elevated PSA levels or abnormal findings on digital rectal examination. As these patients generally had higher PSA values and suspicious clinical findings, their inclusion may have contributed to selection bias. Although the study included a relatively large cohort, all data were derived from a single academic tertiary referral center, which may limit the generalizability of the results. On the other hand, all MRI examinations were jointly reassessed by two experienced radiologists, enhancing the reliability of the radiological evaluation. Overall, our findings may provide a useful basis for future research aimed at further investigating and validating the relationship between prostate volume, PSAd, and the detection of csPCa in patients with PI-RADS 3 lesions.

Conclusion

Our results imply that prostatic volume affects PSAd's diagnostic efficacy in predicting csPCa. Our study encourages the use of lower PSAd thresholds in individuals with larger prostate volumes, especially in borderline cases such as PI-RADS 3 lesions, rather than suggesting clear new cut-off values. In this patient group with diagnostic uncertainty, our volume-adjusted interpretation may enhance risk classification and facilitate tailored biopsy decisions.

Ethics

Ethics Committee Approval: The study was approved by our Institutional Ethics Committee of Ankara University (decision no: İ06-596-25, date: 12.08.2025).

Informed Consent: Written informed consent was obtained from all patients before TRUS-guided biopsies.

Acknowledgements

Publication: The results of the study were not published in full or in part in form of abstracts.

Contribution: There is not any contributors who may not be listed as authors.

Footnotes

Authorship Contributions

Surgical and Medical Practices: E.S., S.B., Concept: Ç.A., E.S., S.B., Design: D.K.Ö., Data Collection or Processing: A.F.Ö., A.M., S.E., Analysis or Interpretation: D.K.Ö., E.Ö., N.H., Ç.G., Literature Search: Ç.A., M.A.İ., M.C.K., Writing: Ç.A., E.Ö., N.H.

Conflict of Interest: No conflict of interest was declared by the authors.

Financial Disclosure: The authors declared that this study received no financial support.

Data Availability Statement

The data sets generated and/or analyzed during the current study are not publicly available but can be obtained from the corresponding author upon reasonable request.

References

1. Ahmed HU, El-Shater Bosaily A, Brown LC, et al.; PROMIS study group. Diagnostic accuracy of multi-parametric MRI and TRUS biopsy in prostate cancer (PROMIS): a paired validating confirmatory study. Lancet. 2017;389:815-822.
2. Van Poppel H, Roobol MJ, Chapple CR, et al. Prostate-specific antigen testing as part of a risk-adapted early detection strategy for prostate cancer: European Association of Urology position and recommendations for 2021. Eur Urol. 2021;80:703-711.
3. Grey ADR, Scott R, Shah B, et al. Multiparametric ultrasound versus multiparametric MRI to diagnose prostate cancer (CADMUS): a prospective, multicentre, paired-cohort, confirmatory study. Lancet Oncol. 2022;23:428-438.
4. Schoots IG, Padhani AR. Risk-adapted biopsy decision based on prostate magnetic resonance imaging and prostate-specific antigen density for enhanced biopsy avoidance in first prostate cancer diagnostic evaluation. BJU Int. 2021;127:175-178.
5. Yusim I, Krenawi M, Mazor E, Novack V, Mabjeesh NJ. The use of prostate specific antigen density to predict clinically significant prostate cancer. Sci Rep. 2020;10:20015.
6. Çelikkaleli F, Özden C, Bulut S, et al. Combining multiparametric MRI and PSA density for improved diagnostic accuracy in prostate cancer. 2024;23:111-115.

7. Vickers A, Touijer K. Re: Philip Cornford, Roderick C.N. van den Bergh, Erik Briers, et al. EAU-EANM-ESTRO-ESUR-ISUP-SIOG guidelines on prostate cancer-2024 update. part I: screening, diagnosis, and local treatment with curative intent. Eur Urol 2024;86:148-63.
8. Rajendran I, Lee KL, Thavaraja L, Barrett T. Risk stratification of prostate cancer with MRI and prostate-specific antigen density-based tool for personalized decision making. Br J Radiol. 2024;97:113-119.
9. Choe S, Patel HD, Lanzotti N, et al. MRI vs transrectal ultrasound to estimate prostate volume and PSAD: impact on prostate cancer detection. Urology. 2023;171:172-178.
10. Turkbey B, Rosenkrantz AB, Haider MA, et al. Prostate imaging reporting and data system version 2.1: 2019 update of prostate imaging reporting and data system version 2. Eur Urol. 2019;76:340-351.
11. Epstein JI, Egevad L, Amin MB, Delahunt B, Srigley JR, Humphrey PA; Grading Committee. The 2014 International Society of Urological Pathology (ISUP) consensus conference on Gleason grading of prostatic carcinoma: definition of grading patterns and proposal for a new grading system. Am J Surg Pathol. 2016;40:244-252.
12. Drost FH, Osses D, Nieboer D, et al. Prostate magnetic resonance imaging, with or without magnetic resonance imaging-targeted biopsy, and systematic biopsy for detecting prostate cancer: a cochrane systematic review and meta-analysis. Eur Urol. 2020;77:78-94.
13. Rouvière O, Puech P, Renard-Penna R, et al.; MRI-FIRST Investigators. Use of prostate systematic and targeted biopsy on the basis of multiparametric MRI in biopsy-naive patients (MRI-FIRST): a prospective, multicentre, paired diagnostic study. Lancet Oncol. 2019;20:100-109.
14. Jambor I, Verho J, Ettala O, et al. Validation of IMPROD biparametric MRI in men with clinically suspected prostate cancer: a prospective multi-institutional trial. PLoS Med. 2019;16:e1002813.
15. Maggi M, Panebianco V, Mosca A, et al. Prostate imaging reporting and data system 3 category cases at multiparametric magnetic resonance for prostate cancer: a systematic review and meta-analysis. Eur Urol Focus. 2020;6:463-478.
16. Aslanoğlu A, Saygın H, Öztürk A, et al. Correlation between PSA density and multiparametric prostate MRI in the diagnosis of prostate cancer. Bull Urooncol 2024;23:29-35.
17. Koparal MY, Sözen TS, Karşiyakali N, et al. Should targeted biopsy be performed in patients who have only PI-RADS 3 lesions? Arch Esp Urol. 2022;75:410-415.
18. Robinson E, Kinsella N, Ap Dafydd D, et al. Prostate specific antigen density and clinically-significant prostate cancer: the influence of prostatic volume. Prostate. 2025;85:784-791.
19. Şahin B, Çelik S, Sözen S, et al.; Members of Turkish Urooncology Association. A new parameter to increase the predictive value of multiparametric prostate magnetic resonance imaging for clinically significant prostate cancer in targeted biopsies: lesion density. Prostate Int. 2024;12:145-150.

Original Article

DOI: 10.4274/uob.galenos.2025.2025.8.5

Bull Urooncol 2026;25(1):7-11

Prognostic Impact of Conglomerated Cribriform Morphology in Gleason Score 7 Prostate Adenocarcinoma

Emel Yaldır[1], Nazlı Sena Şeker[1], Ata Özen[2], Mustafa Açıkalın[1], Cavit Can[2], Ertuğrul Çolak[3]

[1]*Eskişehir Osmangazi University Faculty of Medicine, Department of Pathology, Eskişehir, Türkiye*
[2]*Eskişehir Osmangazi University Faculty of Medicine, Department of Urology, Eskişehir, Türkiye*
[3]*Eskişehir Osmangazi University Faculty of Medicine, Department of Bioistatistics, Eskişehir, Türkiye*

Abstract

Objective: Cribriform architecture has increasingly been recognized as an adverse morphological feature in prostate adenocarcinoma. The present study aimed to describe a novel histopathological subtype of cribriform architecture, termed conglomerated cribriform morphology (CCM), and to investigate its association with clinicopathological parameters and oncological outcomes.
Materials and Methods: Radical prostatectomy specimens with Gleason score 7 and cribriform architecture were retrospectively reviewed. All cases were re-evaluated and categorized into two morphological groups: basic cribriform morphology and CCM. Clinicopathological variables and survival outcomes were compared between these groups.
Results: A total of 151 patients were included in the study, with a mean age of 67.6 years. CCM was detected in 21.2% of cases. This pattern was significantly associated with higher prostate-specific antigen levels, extraprostatic extension, lymph node metastasis, biochemical recurrence, and distant metastasis. Multivariate Cox regression analysis revealed tertiary Gleason pattern, lymphovascular invasion, and CCM as independent predictors of biochemical recurrence. Patients with CCM had significantly shorter biochemical recurrence-free survival.
Conclusion: Cribriform architecture is widely considered an unfavorable feature in prostate cancer. The newly described conglomerated cribriform subtype appears to be a particularly aggressive variant. Recognition of this morphology may contribute to improved prognostic stratification and influence clinical management strategies.
Keywords: Prostate adenocarcinoma, Gleason score 7, cribriform morphology, basic cribriform, conglomerated cribriform, biochemical recurrence

Introduction

In recent years, cribriform architecture has attracted considerable attention in prostate cancer research due to its association with unfavorable clinical outcomes. Several studies have demonstrated that tumors exhibiting cribriform growth patterns behave more aggressively compared with other Gleason pattern 4 morphologies (1-5). The International Society of Urological Pathology (ISUP) describes cribriform carcinoma as a confluent epithelial proliferation composed of malignant cells forming multiple gland-like luminal spaces that are clearly visible at low magnification and lack intervening stroma (6). Distinguishing invasive cribriform carcinoma from intraductal carcinoma of the prostate is an important diagnostic consideration. Intraductal carcinoma generally retains a surrounding basal cell layer, whereas invasive cribriform carcinoma lacks basal cells.

Beyond the simple presence of cribriform glands, several investigators have attempted to determine whether additional morphological characteristics may further refine prognostic assessment. In particular, gland size has been proposed as a potentially relevant parameter. Some reports suggest that larger cribriform glands are associated with worse clinical outcomes, whereas other studies have not confirmed this relationship, leading to ongoing debate regarding the prognostic significance of gland size (7,8). A recent study suggested that cribriform glands larger than 0.25 mm are correlated with adverse prognostic parameters (9).

Although diagnostic challenges exist, cribriform morphology is generally considered to demonstrate relatively good interobserver reproducibility compared with other Gleason pattern 4 patterns (10,11). Morphological features such as

Cite this article as: Yaldır E, Şeker NS, Özen A, Açıkalın M, Can C, Çolak E. Prognostic impact of conglomerated cribriform morphology in Gleason score 7 prostate adenocarcinoma. Bull Urooncol. 2026;25(1):7-11.

Address for Correspondence: Emel Yaldır, Asst. Prof., Eskişehir Osmangazi University Faculty of Medicine, Department of Pathology, Eskişehir, Türkiye
E-mail: emelyaldir@gmail.com **ORCID:** orcid.org/0000-0001-7297-9869
Received: 20.08.2025 **Accepted:** 23.12.2025 **Publication Date:** 18.03.2026

transluminal bridging and reduced peripheral luminal space have been proposed as useful criteria for recognizing cribriform carcinoma (12).

Most published studies have focused on the presence or size of cribriform glands or on differentiating invasive cribriform carcinoma from intraductal carcinoma. However, the potential heterogeneity within invasive cribriform architecture itself has not been extensively investigated. The present study aimed to evaluate distinct histopathological subtypes of invasive cribriform morphology and to assess their potential prognostic significance.

Materials and Methods

Patients who underwent radical prostatectomy between 2010 and 2020 and were diagnosed with Gleason score (GS) 7 (3+4 or 4+3) prostate adenocarcinoma were reviewed retrospectively. Only cases demonstrating cribriform architecture were included in the study. Ethical approval was obtained from the Eskişehir Osmangazi University Faculty of Medicine Non-Invasive Clinical Research Ethics Committee (decision no: 47, date: 27.01.2021, number: E-25403353-050.99-203691).

Pathological Evaluation

All histopathological slides were independently reviewed in a blinded manner by two experienced pathologists. After re-evaluation, 151 cases demonstrating cribriform morphology were included in the study. Data collected included GS, ISUP grade group (GG), presence of a tertiary pattern, lymphovascular and perineural invasion, extraprostatic extension (EPE), seminal vesicle invasion, pathological stage (pT), and lymph node metastasis.

Cribriform architecture was identified according to ISUP criteria (6). Cases were subsequently categorized into two morphological subgroups: basic cribriform morphology (BCM) and conglomerated cribriform morphology (CCM). The presence of even a single, invasive, conglomerated cribriform structure was considered sufficient for classification as CCM. To differentiate invasive cribriform carcinoma from intraductal carcinoma, p63 immunohistochemistry was performed in selected cases. BCM was defined as cribriform glands with round, oval, or irregular contours, clearly separated from the surrounding stroma (Figure 1). CCM was defined as large, invasive cribriform structures demonstrating expansile or infiltrative growth, frequently forming merged glandular masses and occasionally being associated with stromal or capillary components (Figure 2).

Clinical Evaluation

Clinical variables included preoperative prostate-specific antigen (PSA) level, follow-up duration, adjuvant radiotherapy, distant metastasis, biochemical recurrence, biochemical recurrence-free survival (BRFS), disease-related mortality (DRM), and survival status. Biochemical recurrence was defined as a PSA level ≥0.2 ng/mL at least 8 weeks after surgery.

Immunohistochemistry

Sections were prepared from formalin-fixed, paraffin-embedded tissue blocks. After deparaffinization and rehydration, endogenous peroxidase activity was blocked using hydrogen peroxide. Antigen retrieval was performed using Tris-EDTA buffer. Slides were incubated with monoclonal p63 antibody and visualized using an EnVision detection system. Hematoxylin was used for counterstaining. The absence of basal cell staining around cribriform glands supported the diagnosis of invasive carcinoma.

Statistical Analysis

The Shapiro-Wilk test was used to evaluate the distribution of continuous variables. The Mann-Whitney U test was applied for comparisons between groups. Associations between categorical variables were assessed using Pearson's chi-square test, the Yates-corrected chi-square test, or Fisher's exact test, as appropriate. BRFS was analyzed using Kaplan-Meier survival analysis with the log-rank test. Multivariate Cox proportional hazards regression was performed to identify independent predictors of recurrence. A p-value <0.05 was considered statistically significant. Statistical analyses were conducted using IBM SPSS Statistics version 25.

Results

Patient Characteristics

The study included 151 patients. Among these cases, 62.9% were classified as GG2 and 37.1% as GG3. The mean patient age was 67.6 years (range 52-83 years). Pathological staging revealed 33.7% pT2, 41.1% pT3a, and 25.2% pT3b. The mean PSA level was 15.8 ng/mL (range 3-181.9). Perineural invasion was observed in 66.2% of cases, while lymphovascular invasion was present in 25.2%. Positive surgical margins were detected in 29.1% of patients. Among the 129 patients who underwent

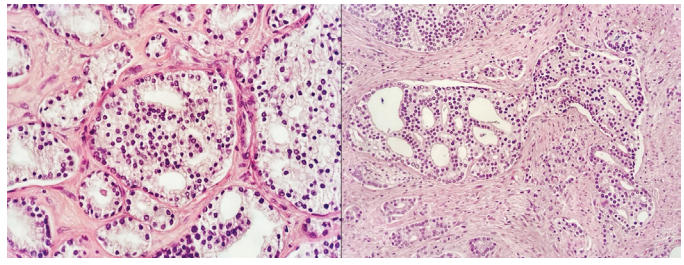

Figure 1. Example of invasive BCM, H&E

BCM: Basic cribriform morphology, H&E: Hematoxylin and eosin

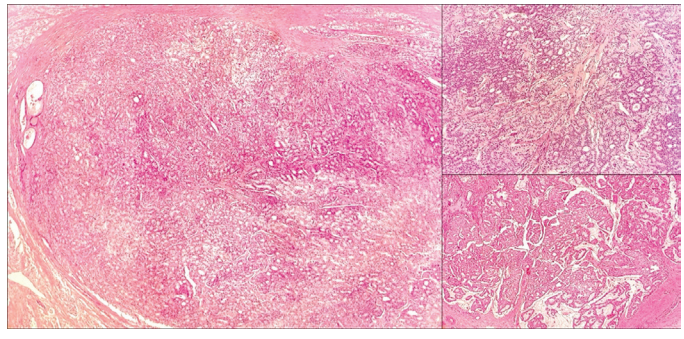

Figure 2. Example of invasive CCM, H&E

CCM: Conglomerated cribriform morphology, H&E: Hematoxylin and eosin

lymph node dissection, lymph node metastasis was identified in 22.5% of patients.

Cribriform Morphology

BCM was detected in 78.8% of cases, while CCM was identified in 21.2%. Most BCM cases (73.9%) were in GG2, whereas 78.1% of CCM cases were in GG3 (p<0.001). The mean cribriform gland percentage was 13.2% in BCM and was significantly higher at 42.8% in CCM (p<0.001). Preoperative PSA ≥10 ng/mL was observed in 45.4% of BCM and 75% of CCM cases (p=0.005). Mean PSA values were 12.8 ng/mL in BCM and 26.5 ng/mL in CCM (p<0.001). EPE was more frequent in CCM (84.4% vs. 61.3%, p=0.025). Surgical margin positivity was also higher in CCM (46.9%, p=0.023). Biochemical recurrence occurred in 62.5% of CCM patients (p<0.001). Lymph node metastasis was significantly more common in CCM (p=0.046). Distant metastases occurred in 5.3% of BCM cases and 34.4% of CCM cases (p<0.001). Although tertiary patterns were more frequent in CCM (18.8% vs. 14.3%), this difference was not statistically significant (p=0.581). Table 1 summarizes the associations between cribriform morphological subtypes and the evaluated prognostic parameters.

Survival Analysis

Radiotherapy was administered to 25.5% of patients. Distant metastasis developed in 11.6% of patients, and biochemical recurrence developed in 31%. Six patients lacked follow-up data. The mean follow-up period was 68 months (range 12-153 months). DRM occurred in 1.4% of patients. Kaplan-Meier analysis demonstrated that BRFS was significantly shorter in CCM than in BCM (51.2 vs. 117.9 months, p<0.001). BRFS in CCM was 3.87-fold shorter than in BCM (Figure 3). Multivariate analysis identified lymphovascular invasion, tertiary pattern, and CCM as independent predictors of recurrence (Table 2).

Discussion

The Gleason grading system remains one of the most important prognostic indicators in prostate adenocarcinoma. Moreover, it serves as a primary method for guiding the selection of optimal therapeutic strategies for patients. Gleason pattern 4 encompasses several architectural patterns including poorly formed glands, fused glands, glomeruloid structures, and CM (13). While these morphological subtypes were not routinely reported in the past, recent studies have consistently shown that invasive CM carries worse prognostic implications (1,3,8,14). In radical prostatectomy specimens with a GS of 7, the presence of cribriform architecture has been linked to reduced 5-year BRFS (7). Consequently, both the Genitourinary Pathology Society and the ISUP now recommend documenting CM in prostate biopsies and radical prostatectomies (15,16).

Although some studies suggest that large cribriform glands are associated with poor prognosis (7), others have reported that size does not matter (8,17). The concept of expansile cribriform architecture has also been proposed to describe large cribriform structures with numerous luminal spaces or dimensions exceeding those of adjacent benign glands. These lesions have been associated with increased rates of EPE, lymph node metastasis, and seminal vesicle invasion (18). While a recent study described cribriform diameter >0.25 mm as a potential prognostic marker, morphological features of the glands were not addressed (9). Importantly, most of these studies did not exclude intraductal carcinoma, and a standard definition for large, small, or expansile cribriform glands has yet to be established.

While earlier studies mainly evaluated the prognostic role of cribriform architecture in GS7 tumors, subsequent research has demonstrated that this architectural pattern retains independent prognostic significance in higher-grade prostate cancers, including GS8 and 9-10 (4,8,19). In addition to morphological differences, cribriform prostate carcinoma has been shown to harbor distinct molecular alterations. These include increased

Table 1. Relationship between the cribriform pattern subgroups and other prognostic parameters

	Basic cribriform pattern (n=119)	Conglomerated cribriform pattern (n=32)	p-value
ISUP group grade n (%)			
2	88 (73.9)	7 (21.9)	**<0.001***
3	31 (26.1)	25 (78.1)	
PSA value n (%)			
<10 ng/mL	65 (54.6)	8 (25)	**0.005***
≥10 ng/mL	54 (45.4)	24 (75)	
PSA value, mean (ng/mL) 95% CI	12.89 11.09-14.69	26.59 15.06-38.13	**<0.001****
Extraprostatic extension n (%)			
Present	73 (61.3)	27 (84.4)	**0.025***
Absent	46 (38.7)	5 (15.6)	
Surgical margin n (%)			
Positive	29 (24.4)	15 (46.9)	**0.023***
Negative	90 (75.6)	17 (53.1)	
Lymphovascular invasion n (%)			
Present	23 (19.3)	15 (46.9)	**0.003***
Absent	96 (80.7)	17 (53.1)	
Tertiary pattern n (%)			
Present	17 (14.3)	6 (18.8)	**0.581*****
Absent	102 (85.7)	26 (81.3)	
Biochemical recurrence n (%)			
Present	25 (22.1)	20 (62.5)	**<0.001***
Absent	88 (77.9)	12 (37.5)	
Lymph node metastasis n (%)			
Present	18 (17.6)	11 (36.7)	**0.046*****
Absent	81 (82.4)	19 (63.3)	
Distant organ metastasis n (%)			
Present	6 (5.3)	11 (34.4)	**<0.001*****
Absent	108 (94.7)	21 (65.6)	

*: Yates test, **: Mann-Whitney U test, ***: Fisher's exact test, CI: Confidence interval, PSA: Prostate-specific antigen

frequencies of PTEN and p27 loss, as well as changes affecting DNA repair pathways (20). Moreover, key genetic changes implicated in cribriform prostate cancer involve deregulation of the MYC, mTORC1, MAPK, KRAS, JAK-STAT, and epidermal growth factor receptor pathways. Epigenetic modifications may further contribute to this deregulation, as cribriform morphology has been linked to increased EZH2 expression and heightened levels of DNA methylation (20-22).

Our study aimed to define histopathological subgroups of invasive CM that may have prognostic significance, particularly in GG2 and GG3 cases where treatment strategies may vary. For routine use, we selected key histopathological criteria that are frequently used to define morphological subtypes. CCM was statistically associated with higher GG, increased EPE, positive surgical margins, advanced pT stage, lymph node metastasis, elevated PSA, biochemical recurrence, and distant metastasis compared with BCM.

Although CM demonstrates the highest interobserver reproducibility among Gleason pattern 4 morphologies (54-79%), diagnostic variability persists (10). Cribriform carcinoma consists of cohesive epithelial sheets forming rounded or irregular trabeculae with multiple lumina. However, this definition does not clearly distinguish CM from complex fused glands, papillary proliferations, glomeruloid growth, or tumors with cribriform-like mucinous morphology. van Leenders et al. (23) defined CM as tumor cell sheets with minimal stromal contact, limited peripheral luminal space, and clearly visible lumina on H&E sections. Shah et al. (12) identified consensus diagnostic criteria including transluminal bridging, lack of stromal contact, absence of intraglandular mucin, <50% peripheral luminal space, and dense cellular proliferation. Parameters with higher disagreement included partial bridging, stromal contact, mucinous fibroplasia, glomeruloid-like patterns, and >50% peripheral luminal space (12). In our study, we applied simplified and well-defined criteria to minimize diagnostic variability. Nevertheless, further studies are required to achieve higher interobserver concordance. Additionally, distinguishing BCM, which is more common in GG2, from intraductal carcinoma or cribriform PIN remains challenging without immunohistochemical basal cell markers. Many prognostic studies on CM do not address this distinction.

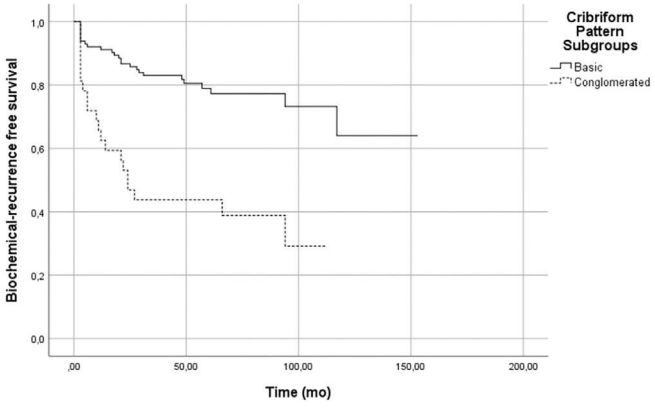

Figure 3. BRFS curves for patients with GG2 and 3 disease, categorized according to the morphology of invasive cribriform glands (BCM vs. CCM) (p<0.001)

BRFS: Biochemical recurrence-free survival, GG: Grade group, BCM: Basic cribriform morphology, CCM: Conglomerated cribriform morphology

Table 2. Cox regression analysis of biochemical recurrence-free survival in patients with GG2 or 3 prostate cancer with invasive cribriform pattern

Multivariate analysis	Hazard ratio (95% CI)	p-value
Cribriform morphology Basic Conglomerated	(Reference) 2.97 (1.59-5.55)	**0.001**
Lymphovascular invasion Absent Present	(Reference) 2.95 (1.55-5.62)	**0.001**
Tertiary pattern Absent Present	(Reference) 3.14 (1.59-6.19)	**0.001**

GG: Grade group, CI: Confidence interval

Study Limitations

This study has several limitations. First, the study was conducted at a single institution and included a relatively small number of cases. Second, the follow-up period was limited for some patients. Because this is the first study describing this morphological subtype, comparative data in the literature are limited. Larger multicenter studies with longer follow-up periods are necessary to validate these findings.

Conclusion

This study represents the first attempt to evaluate the prognostic significance of histopathological subgroups within invasive CM. Our findings suggest that CCM is associated with aggressive tumor behavior, including higher rates of lymph node metastasis and biochemical recurrence, and poorer BRFS. Identification of this morphological pattern in prostate biopsies or prostatectomy specimens may provide valuable prognostic information, particularly in patients with GG2 and 3 disease. Recognition of this subtype could influence treatment planning and follow-up strategies. Further large-scale studies are required to confirm these observations.

Ethics

Ethics Committee Approval: Ethical approval was obtained from the Eskişehir Osmangazi University Faculty of Medicine Non-Invasive Clinical Research Ethics Committee (decision no: 47, date: 27.01.2021, number: E-25403353-050.99-203691).

Informed Consent: Retrospective study.

Acknowledgements

Publication: The results of the study were not published in full or in part in form of abstracts.

Contribution: There is not any contributors who may not be listed as authors.

Footnotes

Authorship Contributions

Surgical and Medical Practices: A.Ö., C.C., Concept: E.Y., N.S.Ş., Design: E.Y., N.S.Ş., Data Collection or Processing: E.Y., N.S.Ş.,

A.Ö., Analysis or Interpretation: E.Y., E.Ç., Literature Search: E.Y., M.A., Writing: E.Y., M.A.

Conflict of Interest: No conflict of interest was declared by the authors.

Financial Disclosure: The authors declared that this study received no financial support.

References

1. Kweldam CF, Wildhagen MF, Steyerberg EW, Bangma CH, van der Kwast TH, van Leenders GJ. Cribriform growth is highly predictive for postoperative metastasis and disease-specific death in Gleason score 7 prostate cancer. Mod Pathol. 2015;28:457-464.
2. Keefe DT, Schieda N, El Hallani S, et al. Cribriform morphology predicts upstaging after radical prostatectomy in patients with Gleason score 3 + 4 = 7 prostate cancer at transrectal ultrasound (TRUS)-guided needle biopsy. Virchows Arch. 2015;467:437-442.
3. Kweldam CF, Kümmerlin IP, Nieboer D, et al. Presence of invasive cribriform or intraductal growth at biopsy outperforms percentage grade 4 in predicting outcome of Gleason score 3+4=7 prostate cancer. Mod Pathol. 2017;30:1126-1132.
4. Kweldam CF, Kümmerlin IP, Nieboer D, et al. Disease-specific survival of patients with invasive cribriform and intraductal prostate cancer at diagnostic biopsy. Mod Pathol. 2016;29:630-636.
5. Masoomian M, Downes MR, Sweet J, et al. Concordance of biopsy and prostatectomy diagnosis of intraductal and cribriform carcinoma in a prospectively collected data set. Histopathology. 2019;74:474-482.
6. van der Kwast TH, van Leenders GJ, Berney DM, et al. ISUP consensus definition of cribriform pattern prostate cancer. Am J Surg Pathol. 2021;45:1118-1126.
7. Hollemans E, Verhoef EI, Bangma CH, et al. Large cribriform growth pattern identifies ISUP grade 2 prostate cancer at high risk for recurrence and metastasis. Mod Pathol. 2019;32:139-146.
8. Iczkowski KA, Torkko KC, Kotnis GR, et al. Digital quantification of five high-grade prostate cancer patterns, including the cribriform pattern, and their association with adverse outcome. Am J Clin Pathol. 2011;136:98-107.
9. Chan E, McKenney JK, Hawley S, et al. Analysis of separate training and validation radical prostatectomy cohorts identifies 0.25 mm diameter as an optimal definition for "large" cribriform prostatic adenocarcinoma. Modern Pathology. 2022;35:1092-1100.
10. Kweldam CF, Nieboer D, Algaba F, et al. Gleason grade 4 prostate adenocarcinoma patterns: an interobserver agreement study among genitourinary pathologists. Histopathology. 2016;69:441-449.
11. van der Slot MA, Hollemans E, den Bakker MA, et al. Inter-observer variability of cribriform architecture and percent Gleason pattern 4 in prostate cancer: relation to clinical outcome. Virchows Arch. 2021;478:249-256.
12. Shah RB, Cai Q, Aron M, et al. Diagnosis of "cribriform" prostatic adenocarcinoma: an interobserver reproducibility study among urologic pathologists with recommendations. Am J Cancer Res. 2021;11:3990-4001.
13. Epstein JI, Egevad L, Amin MB, et al. The 2014 International Society of Urological Pathology (ISUP) consensus conference on Gleason grading of prostatic carcinoma. Am J Surg Pathol. 2016;40:244-252.
14. Kir G, Sarbay BC, Gümüş E, Topal CS. The association of the cribriform pattern with outcome for prostatic adenocarcinomas. Pathol Res Pract. 2014;210:640-644.
15. van Leenders GJLH, van der Kwast TH, Grignon DJ, et al.; ISUP Grading Workshop Panel Members. The 2019 International Society of Urological Pathology (ISUP) consensus conference on grading of prostatic carcinoma. Am J Surg Pathol. 2020;44:e87-e99.
16. Epstein JI, Amin MB, Fine SW, et al. The 2019 Genitourinary Pathology Society (GUPS) white paper on contemporary grading of prostate cancer. Arch Pathol Lab Med. 2021;145:461-493.
17. Rijstenberg LL, Hansum T, Kweldam CF, et al. Large and small cribriform architecture have similar adverse clinical outcome on prostate cancer biopsies. Histopathology. 2022;80:1041-1049.
18. Greenland NY, Cowan JE, Zhang L, et al. Expansile cribriform Gleason pattern 4 has histopathologic and molecular features of aggressiveness and greater risk of biochemical failure compared to glomerulation Gleason pattern 4. Prostate. 2020;80:653-659.
19. Harding-Jackson N, Kryvenko ON, Whittington EE, et al. Outcome of Gleason 3 + 5 = 8 prostate cancer diagnosed on needle biopsy: prognostic comparison with Gleason 4 + 4 = 8. J Urol. 2016;196:1076-1081.
20. Elfandy H, Armenia J, Pederzoli F, et al. Genetic and epigenetic determinants of aggressiveness in cribriform carcinoma of the prostate. Mol Cancer Res. 2019;17:446-456.
21. Böttcher R, Kweldam CF, Livingstone J, et al. Cribriform and intraductal prostate cancer are associated with increased genomic instability and distinct genomic alterations. BMC Cancer. 2018;18:8.
22. Xiao GQ, Nguyen E, Unger PD, Sherrod AE. Comparative expression of immunohistochemical biomarkers in cribriform and pattern 4 non-cribriform prostatic adenocarcinoma. Exp Mol Pathol. 2020;114:104400.
23. van Leenders GJLH, Verhoef EI, Hollemans E. Prostate cancer growth patterns beyond the Gleason score: entering a new era of comprehensive tumour grading. Histopathology. 2020;77:850-861.

Original Article

DOI: 10.4274/uob.galenos.2025.2025.10.2

Bull Urooncol 2026;25(1):12-17

What Changed in Partial Nephrectomy in the Last Decade? A Comparison of Surgical Management and Outcomes

Oktay Üçer[1], Talha Müezzinoğlu[1], Murat Gülşen[2], Çağrı Akpınar[3], Sertaç Yazıcı[4], Serhat Çetin[5], Oğuzcan Erbatu[1], Volkan İzol[6]

[1]*Manisa Celal Bayar University Faculty of Medicine, Department of Urology, Manisa, Türkiye*
[2]*Ondokuz Mayıs University Faculty of Medicine, Department of Urology, Samsun, Türkiye*
[3]*Ankara University Faculty of Medicine, Department of Urology, Ankara, Türkiye*
[4]*Hacettepe University Faculty of Medicine, Department of Urology, Ankara, Türkiye*
[5]*Gazi University Faculty of Medicine, Department of Urology, Ankara, Türkiye*
[6]*Çukurova University Faculty of Medicine, Department of Urology, Ankara, Türkiye*

Abstract

Objective: Surgical management of renal tumors has shifted toward partial nephrectomy (PN), even in larger or more complex cases. This study aimed to evaluate how clinical practice patterns, surgical approaches, and outcomes of PN evolved over the last decade.
Materials and Methods: Using the Turkish Urooncology Association REDCap database, we retrospectively reviewed 3,482 patients who underwent PN for renal cell carcinoma between 1997 and 2024. Patients were stratified into earlier (before 2014) and later (after 2014) groups. Demographic, surgical, perioperative, and oncologic parameters were compared. Subgroup analyses assessed open, laparoscopic, and robot-assisted PN. Statistical analyses were performed using t-tests and chi-square tests with significance set at $p<0.05$.
Results: Patients in the last decade were older (56.9 vs. 54.9 years; $p<0.001$). Hospital stay, blood loss, and ischemia time were significantly reduced (all $p<0.001$). The use of minimally invasive PN increased significantly, with robotic procedures comprising 12.2% of cases after 2014 ($p<0.001$). Intraoperative complications declined from 3.5% to 1.5% ($p=0.001$), and postoperative complications declined from 14.1% to 6.5% ($p<0.001$). Recurrence decreased from 8.7% to 3.5% ($p<0.001$), while positive margin rates remained stable at 9.1% in both groups. Subgroup analyses confirmed reductions in complications and in recurrence for both open and laparoscopic PN.
Conclusion: PN has evolved toward wider use in older patients and with minimally invasive techniques. Despite comparable tumor sizes, perioperative complications and recurrence rates declined significantly over time, supporting PN as a safe and effective treatment for complex renal tumors.
Keywords: Nephrectomy, renal cell carcinoma, surgical oncology

Introduction

Recently, surgical management of renal tumors has increasingly shifted toward partial rather than radical nephrectomy (RN), even for larger and more complex cases when feasible (1,2). Earlier detection through imaging and growing experience with partial nephrectomy (PN) have influenced this shift (3,4). PN is widely accepted as the preferred option for T1a renal masses and is increasingly used in selected T1b and even T2 cases when technically possible (5,6). Although RN was more common in the past, its use in T1 and selected T2 tumors has gradually decreased (7,8). PN offers similar cancer control especially for T1 tumors and may help preserve long term kidney function more effectively (9). However particularly in larger tumors, some studies have reported mixed results regarding overall survival, keeping the discussion open (9,10). With advances in surgical techniques and increased use of minimally invasive methods, open, laparoscopic and robot assisted PN have become more common and safer in many centers (11,12). Studies support the use of PN for larger renal tumors, showing advantages in kidney function outcomes, though with a slightly higher rate of complications (13,14). Also, the oncologic impact of positive surgical margins (PSM), a concerning outcome of PN, remains

Cite this article as: Üçer O, Müezzinoğlu T, Gülşen M, et al. What changed in partial nephrectomy in the last decade? A comparison of surgical management and outcomes. Bull Urooncol. 2026;25(1):12-17.

Address for Correspondence: Oğuzcan Erbatu Asst. Prof., Manisa Celal Bayar University Faculty of Medicine, Department of Urology, Manisa, Türkiye
E-mail: oguzcan90@gmail.com **ORCID:** orcid.org/0000-0002-2840-0028
Received: 08.10.2025 **Accepted:** 27.11.2025 **Publication Date:** 18.03.2026

controversial (15). For small renal tumors, management may include PN as previously discussed, as well as ablative techniques or active surveillance in selected patients (16,17). This diversity in the management of renal tumors maintains the topic's relevance.

Our study aims to assess how the clinical approach to PN has changed over time by comparing patients treated in the last decade with those from earlier years. We investigated shifts in patient selection, surgical techniques, tumor complexity, and perioperative and oncological outcomes.

Materials and Methods

In our study, data from the Turkish Urooncology Association REDCap database were retrospectively reviewed (18,19). A total of 3,482 patients who underwent PN for renal cell carcinoma between 1997 and 2024 were included. As this was a multicenter, retrospective study, variability in surgical expertise, available technology, and institutional protocols was inevitable. However, all participating centers are high-volume tertiary institutions experienced in renal surgery, and data entry followed standardized definitions within the national database. While some heterogeneity may exist, the large sample size and consistent data collection likely reduce its overall impact. Variables assessed included patient age at the time of surgery, tumor size, operation type and duration, preoperative nephrometry scores, length of hospital stay, ischemia duration, and complications. Injuries involving the bowel, major vascular structures, diaphragm, or liver were collectively categorized as intraoperative complications and recorded as present or absent. Postoperative complications were similarly recorded as binary variables and included bleeding or the need for selective embolization, urinary fistula or the associated need for ureteral stenting, postoperative renal failure, reoperation, and development of deep vein thrombosis or pulmonary embolism. During postoperative follow-up, surgical margin status and tumor recurrence were also documented.

All statistical analyses were performed to compare clinical, surgical, and oncologic parameters between patients treated before 2014 and patients treated after 2014. That year was chosen as the cut-off point to provide a balanced comparison between earlier and more recent cases and to represent the most recent decade of data. It was not linked to any specific guideline change or technological milestone, but aimed instead to reflect temporal improvements in surgical practice and institutional experience. Continuous variables were expressed as mean ± standard deviation and compared using independent samples t-tests. Categorical variables were summarized as frequencies and percentages, and comparisons were performed using Pearson's chi-square test. Subgroup analyses were conducted for patients who underwent open, laparoscopic, or robot-assisted PN to assess changes over time in complication rates, recurrence, and surgical margin status.

Statistical Analysis

Statistical analyses were performed using IBM SPSS Statistics version 29.0 (IBM Corp., Armonk, NY, USA). A p-value of less than 0.05 was considered statistically significant. Figures were generated using Python version 3.14.0 (Python Software Foundation, Wilmington, DE, USA).

Ethical approval for this multicenter database study was obtained from the Institutional Ethics Committee of Manisa Celal Bayar University (decision no: 20.478.486/3395, date: 04.09.2025). All participating centers have the necessary approvals to enter patient data into the database, and all data are stored anonymously.

Results

Significant differences between the earlier patients (before 2014) and patients from the last decade (after 2014) were observed using independent-samples t-tests. The last-decade patients were significantly older compared to earlier patients (56.92±14.12 vs. 54.92±13.03; p<0.001). Length of hospital stay (4.24±7.99 vs. 5.47±7.77; p<0.001), estimated blood loss (195.35±250.43 vs. 237.34±279.85; p < 0.001), and ischemia time (17.06±0.7 vs. 19.38±0.8; p<0.001) were all significantly lower in the last-decade patients. No statistically significant differences were found between the groups in terms of tumor size (3.65±2.01 vs. 3.82±2.38; p=0.78) and operative time (2.23±1.44 vs. 2.35±0.91; p=0.14) (Table 1). The narrow standard deviation, especially for ischemia time, is likely due to standardized reporting across centers and to the fact that extreme values were both infrequent and excluded.

Preoperative nephrometry scores were assessed using the RENAL, PADUA, C-index, and DAP systems in 670, 319, 116, and 117 patients, respectively. The limited number of patients with available nephrometry scores was due to the retrospective design the long study period, and the multicenter nature of the study. Nevertheless, extensive data screening was performed to include the maximum number of eligible cases, and the final analyses were based on these data. While mean RENAL (6.97 vs.

Table 1. Comparison of patient, tumor and perioperative characteristics

Variable	Before 2014	After 2014	p-value
Age (years)	54.92±13.03	56.92±14.12	**<0.001**
Hospital stays (days)	5.47±7.77	4.24±7.99	**<0.001**
Estimated blood loss (mL)	237.34±279.85	195.35±250.43	**<0.001**
Ischemia time (minutes)	19.38±0.8	17.06±0.7	**<0.001**
Tumor size (cm)	3.82±2.38	3.65±2.01	0.780
Operative time (hours)	2.35±0.91	2.23±1.44	0.140

6.54) and PADUA (8.66 vs. 8.35) scores were slightly higher in patients in the last decade, these differences were not statistically significant (p=0.123 and 0.147, respectively). The C-index was marginally higher in earlier patients (2.09 vs. 1.94), whereas DAP scores were slightly higher in the last-decade group (6.15 vs. 5.91); neither difference reached statistical significance (p=0.777 and 0.374, respectively) (Table 2).

A significant shift in the type of surgical approach was observed between the two groups. Among earlier patients, 618 (71.2%) underwent open surgery and 250 (28.8%) laparoscopic surgery. In the last decade, 1,280 patients (49%) underwent open surgery, 1,016 (38.8%) underwent laparoscopic surgery, and 318 (12.2%) underwent robot-assisted surgery. This change was statistically significant according to Pearson's chi-square test (p<0.001) (Figure 1). Significant differences were observed in intraoperative and postoperative complications and in recurrence rates. Intraoperative complications were recorded in 29 patients (3.5%) in the earlier cohort and in 37 patients (1.5%) in the last-decade cohort (p=0.001). Postoperative complications were also more frequent in the earlier group, affecting 116 patients (14.1%) compared with 165 patients (6.5%) in the last-decade group (p<0.001). There was no statistically significant difference in PSM; both groups had identical rates of 9.1% (p=1.000). Recurrence rates significantly declined from 8.7% (77 cases) in the earlier group to 3.5% (92 cases) in the last-decade group (p<0.001) (Table 3).

A subgroup analysis was conducted focusing only on patients who underwent open PN. Significant differences were identified in intraoperative and postoperative complications, as well as in recurrence. Intraoperative complications were recorded in 3.1% (18/578) of patients in the earlier period and 1.4% (17/1227) of patients in the last decade (p=0.001). Postoperative complications occurred in 10.9% (63/576) of earlier patients and in 5.5% (67/1224) of patients from the last decade (p<0.001). No statistically significant difference in surgical margin status was found: positive margins were reported in 8.0% (47/591) of patients in the earlier period and 9.4% (22/234) of patients in the last decade (p=0.300). Recurrence was detected in 8.1% (50/618) of earlier patients and in 3.5% (45/1280) of patients from the last decade (p<0.001), indicating a significant reduction over time (Table 3).

A secondary subgroup analysis was then performed, focusing on patients who underwent laparoscopic PN. Significant differences were observed between the two groups in intraoperative and postoperative complications and recurrence rates. Intraoperative complications occurred in 3.9% (9/233) of patients from an earlier period and 1.5% (19/1275) of patients from the last decade (p<0.05). Postoperative complications were noted in 19.4% (45/232) of patients from an earlier period and in 7.3% (94/1288) of patients from the last decade (p<0.001). No statistically significant difference in surgical margin status was found: positive margins were observed in 12.7% (21/165) of patients from the earlier period and 8.9% (102/1140) of patients from the last decade (p=0.130). Recurrence was reported in 10.0% (25/250) of earlier patients and 3.4% (45/1334) of patients in the last decade, representing a statistically significant decrease (p<0.001). Over the last decade, 318 patients who underwent robot-assisted laparoscopic surgery were included in the laparoscopic group because no robotic surgeries were performed in the earlier group (Table 3).

A subgroup analysis evaluated the relationships among PSM, recurrence, and tumor size by time period. Before 2014, recurrence occurred in 7/54 (13.0%) patients with PSM vs. 70/832 (8.4%) patients with negative surgical margins (p=0.19). After 2014, recurrence was 3/21 (14.3%) vs. 87/2,575 (3.4%) (p=0.07). Mean tumor size was slightly higher in PSM cases both before (4.25±2.34 cm vs. 3.79±2.29 cm; p=0.11) and after 2014 (4.05±1.92 cm vs. 3.63±1.97 cm; p=0.12). Although PSM patients showed higher recurrence rates and larger tumors in both periods, none of these differences were statistically significant.

Discussion

In this study, we observed notable shifts in the surgical management and clinical characteristics of patients undergoing PN over time. The last-decade group was significantly older than earlier patients (p<0.001), and showed significant reductions in length of hospital stay (p<0.001), estimated blood loss (p<0.001), and ischemia time (p<0.001). Despite these factors, perioperative outcomes improved markedly: intraoperative complications declined from 3.5% to 1.5% (p=0.001), postoperative complications declined from 14.1% to 6.5% (p<0.001), and recurrence rates declined from 8.7% to 3.5% (p<0.001). Use of laparoscopic PN rose significantly, from 28.8% to 38.8%, with an additional 12.2% undergoing robot-assisted surgery (p<0.001). Over time, surgical practice shifted from open PN to laparoscopic and robotic PN. Advances in minimally invasive surgery, together with greater surgical expertise, improved hospital protocols, and multidisciplinary care, have led to shorter ischemia times, less blood loss, and fewer complications. These combined factors likely contributed to better perioperative and oncologic outcomes observed over the last decade without increasing PSM.

Support for the oncologic safety of PN in larger tumors is further provided by Janssen et al. (5), who found significantly lower recurrence with PN than with RN for T2 tumors (9.0% vs. 41.6%, p=0.046), along with significantly better cancer specific survival

Table 2. Comparison of nephrometry scores

Score	Total (n)	Before 2014 (mean)	After 2014 (mean)	p-value
RENAL	670	6.54±2.05	6.97±2.01	0.123
PADUA	319	8.35±1.73	8.66±1.89	0.147
C-Index	116	2.09±3.31	1.94±1.14	0.777
DAP	117	5.91±1.46	6.15±1.39	0.374

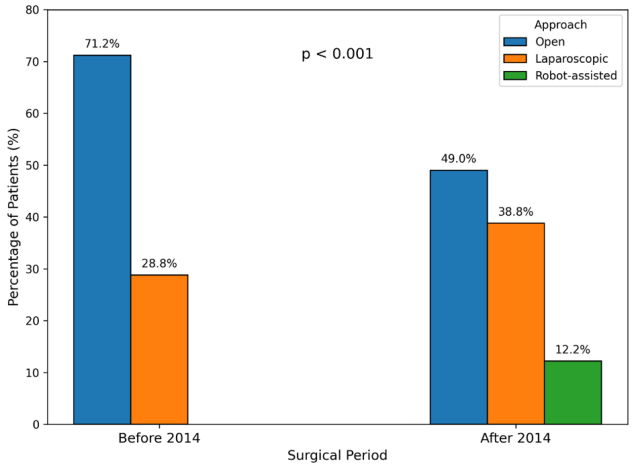

Figure 1. Change in surgical approach over time

in the PN group (p=0.015). However, this difference likely reflects selection bias, as PN was offered electively to carefully selected patients with more favorable tumor characteristics, whereas larger and more aggressive tumors were preferentially treated with RN. In our series, recurrence rates were also lower over the last decade despite comparable tumor sizes, supporting the notion that, with growing surgical expertise, PN can be safely expanded to selected patients without compromising oncologic outcomes.

The systematic review and meta-analysis conducted by Mir et al. (13), which included 21 comparative studies covering patients treated between 1970 and 2012, primarily reflects earlier surgical practice and thus temporally aligns with the first half of our cohort. In their analysis of T1b and ≥T2 tumors, patients selected for PN were on average 2.3 years younger (p<0.001) and had tumors that were 0.65 cm smaller (p<0.001) than those undergoing RN. They also reported a significantly higher overall complication risk in the PN group (odds ratio: 1.74; p<0.001). In contrast, our more recent data show that PN has increasingly been applied to older patients with tumors of similar size, and, importantly, this shift has been accompanied by a marked decline in complication rates, whereas positive margin rates have remained stable. These evolving trends likely reflect improvements in surgical expertise, patient selection, and institutional practices.

Hjelle et al. (20) similarly observed a significant increase in the utilization of PN across Norway between 2008 and 2013. This trend was particularly evident for tumors up to 7 cm and was associated with a corresponding improvement in relative survival rates. PN rates rose from 43% to 66% for tumors ≤4 cm and from 10% to 18% for tumors measuring 4.1-7 cm. The 5-year relative survival for T1b tumors was 98.8% following PN versus 90.0% following RN (p<0.05). Our data reflect this trend, showing a clear rise in minimally invasive and robotic PN over the last decade, while open surgery rates have declined. Importantly, perioperative and oncologic outcomes improved in parallel, with fewer complications and lower recurrence rates, despite the tumors treated being of similar size. These findings suggest that broader implementation of PN can lead to improved outcomes, particularly when performed at experienced centers.

Our findings are further supported by the comprehensive analysis of Touijer et al. (21), who reviewed outcomes of PN across multiple institutions and concluded that PN is both feasible and oncologically safe for tumors >4 cm. In their multicenter cohort, local recurrence rates after PN for T1b tumors were 3.6%, comparable to the 2.3% recurrence observed after RN; disease-specific survival did not differ significantly between the two groups (p=0.800). Moreover, they reported a higher, but acceptable, complication rate in PN for larger tumors, with urinary fistula rates of 4.4% and perioperative bleeding rates of 3.1%. Consistent with these findings, our series demonstrated a decline in recurrence and complication rates over time, reflecting that growing surgical experience and minimally invasive techniques can effectively mitigate the technical challenges of modern PN.

Table 3. Comparison of complications, surgical margins and recurrence by period and surgical technique

Parameter	Surgical type	Before 2014	After 2014	p-value
Intraoperative complications	Overall	29/824 (3.5%)	37/2538 (1.5%)	**0.001**
	Open PN	18/578 (3.1%)	17/1227 (1.4%)	**0.001**
	Laparoscopic PN	9/233 (3.9%)	19/1275 (1.5%)	**<0.05**
Postoperative complications	Overall	116/822 (14.1%)	165/2549 (6.5%)	**<0.001**
	Open PN	63/576 (10.9%)	67/1224 (5.5%)	**<0.001**
	Laparoscopic PN	45/232 (19.4%)	94/1288 (7.3%)	**<0.001**
Surgical margin	Overall	54/591 (9.1%)	21/234 (9.1%)	1.000
	Open PN	47/591 (8.0%)	22/234 (9.4%)	0.300
	Laparoscopic PN	21/165 (12.7%)	102/1140 (8.9%)	0.130
Recurrence	Overall	77/886 (8.7%)	92/2664 (3.5%)	**<0.001**
	Open PN	50/618 (8.1%)	45/1280 (3.5%)	**<0.001**
	Laparoscopic PN	25/250 (10.0%)	45/1334 (3.4%)	**<0.001**

PN: Partial nephrectomy

Study Limitations

This study has several limitations. As a retrospective multicenter study, it was inevitable that there would be variability in surgeon experience, technology availability, and institutional practices. Potential confounders such as comorbidities, tumor location, and incomplete nephrometry data were not adjusted for in the analysis and may have influenced some results. Some long-term renal function outcomes, such as estimated glomerular filtration rate trends, could not be analyzed. Moreover, missing data bias may exist, as nephrometry scores were available only for a subset of patients. Multivariate regression could not be performed due to insufficient variable completeness, which limited our ability to adjust for potential confounders. Despite these limitations, the large sample size and standardized data collection across high-volume tertiary centers enhance the reliability and generalizability of the findings.

Conclusion

Our findings demonstrate significantly lower complication and recurrence rates among patients undergoing PN over the last decade, despite increasing tumor complexity and broader use of minimally invasive techniques. These results suggest that PN remains a safe and effective option even for more complex renal tumors. Ongoing advances in surgical techniques and patient selection remain important for maintaining favorable outcomes.

Ethics

Ethics Committee Approval: Ethical approval for this multicenter database study was obtained from the Institutional Ethics Committee of Manisa Celal Bayar University (decision no: 20.478.486/3395, date: 04.09.2025).

Informed Consent: All participating centers have the necessary approvals to enter patient data into the database, and all data are stored anonymously.

Acknowledgements

Publication: The results of the study were not published in full or in part in form of abstracts.

Contribution: There is not any contributors who may not be listed as authors.

Footnotes

Authorship Contributions

Surgical and Medical Practices: O.Ü., T.M., M.G., Ç.A., S.Y., S.Ç., V.İ., Concept: T.M., M.G., S.Y., Design: T.M., M.G., V.İ., Data Collection or Processing: O.Ü., S.Y., O.E., Analysis or Interpretation: O.Ü., Ç.A., Literature Search: M.G., S.Y., S.Ç., O.E., Writing: O.Ü., O.E.

Conflict of Interest: No conflict of interest was declared by the authors.

Financial Disclosure: The authors declared that this study received no financial support.

References

1. Lasorsa F, Bignante G, Orsini A, et al. Partial nephrectomy in elderly patients: a systematic review and analysis of comparative outcomes. Eur J Surg Oncol. 2024;50:108578.
2. Stout TE, Gellhaus PT, Tracy CR, Steinberg RL. Robotic partial vs radical nephrectomy for clinical T3a tumors: a narrative review. J Endourol. 2023;37:978-985.
3. Gao B, Gorgen ARH, Bhatt R, et al. Avoiding "needless" nephrectomy: what is the role of small renal mass biopsy in 2024? Urol Oncol. 2024;42:236-244.
4. Chen K, Lee A, Huang HH, et al. Evolving trends in the surgical management of renal masses over the past two decades: a contemporary picture from a large prospectively-maintained database. Int J Urol. 2019;26:465-474.
5. Janssen MWW, Linxweiler J, Terwey S, et al. Survival outcomes in patients with large (≥7cm) clear cell renal cell carcinomas treated with nephron-sparing surgery versus radical nephrectomy: Results of a multicenter cohort with long-term follow-up. PLoS One. 2018;13:e0196427.
6. Hadjipavlou M, Khan F, Fowler S, Joyce A, Keeley FX, Sriprasad S; BAUS Sections of Endourology and Oncology. Partial vs radical nephrectomy for T1 renal tumours: an analysis from the British Association of Urological Surgeons Nephrectomy Audit. BJU Int. 2016;117:62-71.
7. Meskawi M, Becker A, Bianchi M, et al. Partial and radical nephrectomy provide comparable long-term cancer control for T1b renal cell carcinoma. Int J Urol. 2014;21:122-128.
8. Rose TL, Kim WY. Renal cell carcinoma: a review. JAMA. 2024;332:1001-1010.
9. Scosyrev E, Messing EM, Sylvester R, Campbell S, Van Poppel H. Renal function after nephron-sparing surgery versus radical nephrectomy: results from EORTC randomized trial 30904. Eur Urol. 2014;65:372-377.
10. Kohada Y, Shikuma H, Goto K, et al. Real-world survival outcomes of partial versus radical nephrectomy: cause-specific and time-dependent effects. Clin Genitourin Cancer. 2025;23:102391.
11. Boy A, Hein J, Bollow M, Lazica D, Roosen A, Ubrig B. Minimal-invasive vs. offene nierenteilresektionen: perioperative erfolgs- und komplikationsraten [Minimally invasive vs. open partial nephrectomy: perioperative success and complication rates]. Urologe A. 2018;57:821-827. German.
12. Cole R, Semerjian A. Robotic partial nephrectomy: techniques for complex tumors. Urol Oncol. 2025;43:461-466.
13. Mir MC, Derweesh I, Porpiglia F, Zargar H, Mottrie A, Autorino R. Partial nephrectomy versus radical nephrectomy for clinical T1b and T2 renal tumors: a systematic review and meta-analysis of comparative studies. Eur Urol. 2017;71:606-617.
14. Al-Qudimat AR, Altahtamouni SB, Elaarag M, et al. Surgical strategies in renal cancer: a meta-analysis of partial vs. radical nephrectomy outcomes across tumor stages. Qatar Med J. 2025;2025:54.
15. Bulut EC, Elmas B, Kaba M, et al. Impact of positive surgical margins on renal cell carcinoma recurrence. Bull Urooncol. 2024;23:68-72.
16. Singh RK, Gideon M, Rajendran R, Mathew G, Nair K. Advancing treatment frontiers: radiofrequency ablation for small renal mass-intermediate-term results. J Kidney Cancer VHL. 2023;10:1-6.
17. Aveta A, Iossa V, Spena G, et al. Ablative treatments for small renal masses and management of recurrences: a comprehensive review. life (basel). 2024;14:450.
18. Harris PA, Taylor R, Thielke R, Payne J, Gonzalez N, Conde JG. Research electronic data capture (REDCap)--a metadata-driven methodology and workflow process for providing translational research informatics support. J Biomed Inform. 2009;42:377-381.
19. Harris PA, Taylor R, Minor BL, et al.; REDCap Consortium. The REDCap consortium: building an international community of software platform partners. J Biomed Inform. 2019;95:103208.

20. Hjelle KM, Johannesen TB, Bostad L, Reisæter LAR, Beisland C. National Norwegian practice patterns for surgical treatment of kidney cancer tumors ≤7cm: adherence to changes in guidelines may improve overall survival. Eur Urol Oncol. 2018;1:252-261.

21. Touijer K, Jacqmin D, Kavoussi LR, et al. The expanding role of partial nephrectomy: a critical analysis of indications, results, and complications. Eur Urol. 2010;57:214-222.

Original Article

DOI: 10.4274/uob.galenos.2026.2025.12.1

Bull Urooncol 2026;25(1):18-26

Prognostic Impact of Intraductal Carcinoma in Patients with Metastatic Prostate Cancer Treated with Abiraterone Acetate or Enzalutamide

Hatice Bölek, Satı Coşkun Yazgan, Emre Yekedüz, Yüksel Ürün

Ankara University Faculty of Medicine, Department of Medical Oncology, Ankara, Türkiye

Abstract

Objective: This study aimed to evaluate the prognostic impact of intraductal carcinoma of the prostate (IDC-P) in patients with metastatic prostate cancer treated with enzalutamide or abiraterone acetate.

Materials and Methods: We retrospectively analyzed data from patients with metastatic prostate cancer who received abiraterone acetate or enzalutamide. The primary outcome was overall survival (OS). Secondary outcomes were prostate-specific antigen (PSA) progression-free survival (PFS) and radiologic PFS.

Results: A total of 94 men were enrolled in the study. Among them, 30 patients (31.9%) received androgen receptor pathway inhibitors for metastatic hormone-sensitive prostate cancer (mHSPC), and 64 patients (68.1%) were treated for metastatic castration-resistant prostate cancer (mCRPC). The presence of IDC-P was associated with significantly shorter OS than in patients without IDC-P (35.38 months vs. 55.59 months, respectively; p=0.011). In mCRPC, median OS was significantly shorter in patients with IDC-P (35.38-55.59 months), while the difference was not significant in the mHSPC cohort [35.48 months vs. not reached (NR)]. Multivariate Cox regression analysis identified IDC-P as an independent adverse prognostic factor for OS (hazard ratio 3.16, 95% confidence interval 1.56-6.41; p=0.001). Similarly, median PSA-PFS was significantly shorter in patients with IDC-P than in those without IDC-P (15.87 vs. 31.11 months, p=0.020). In mCRPC, median PSA-PFS was significantly shorter in patients with IDC-P (15.9 vs. 28.4 months), whereas the difference was not significant in the mHSPC cohort (18.3 months vs. NR).

Conclusion: The presence of IDC-P is associated with poorer PSA-PFS and OS in patients with metastatic prostate cancer treated with abiraterone acetate or enzalutamide.

Keywords: Prostate cancer, intraductal carcinoma, enzalutamide, abiraterone acetate

Introduction

The most frequently observed histological type of prostate cancer is prostatic acinar adenocarcinoma. While the term "ductal spread of prostate carcinoma" has been used for several decades, intraductal carcinoma of prostate (IDC-P) was recognized as a distinct pathological entity in the 2016 edition of the World Health Organization (WHO) classification of tumors of the urinary system and male genital organs (1-3). IDC-P is considered a manifestation of advanced prostate cancer, characterized by intraductal spread of aggressive tumor cells and cancerous transformation of pre-existing ductal and acinar structures by high-grade prostatic adenocarcinoma. IDC-P is identified in approximately 15-30% of radical prostatectomy specimens and 14% of biopsies with concomitant carcinoma, whereas isolated IDC-P without invasive cancer is exceedingly rare, occurring in only 0.06-0.26% of cases (4-7). Presence of IDC-P correlates with a higher tumor grade, larger volume, and advanced stage for localized prostate cancer (8-10). Compared with conventional acinar adenocarcinoma, IDC-P is enriched for genomic alterations linked to aggressive behavior, including *PTEN* loss, *TP53* alterations, and *BRCA2* alterations, along with MYC amplification and higher levels of genomic instability (11-13). IDC-P is associated with a higher risk of biochemical recurrence, as well as shorter prostate cancer-specific survival and overall survival (OS) following definitive treatment (14,15).

Cite this article as: Bölek H, Yazgan SC, Yekedüz E, Ürün Y. Prognostic impact of intraductal carcinoma in patients with metastatic prostate cancer treated with abiraterone acetate or enzalutamide. Bull Urooncol. 2026;25(1):18-26.

Address for Correspondence: Hatice Bölek, MD, Ankara University Faculty of Medicine, Department of Medical Oncology, Türkiye, Ankara
E-mail: hati.kocc@gmail.com **ORCID:** orcid.org/0000-0001-8659-7327
Received: 04.12.2025 **Accepted:** 24.02.2026 **Publication Date:** 18.03.2026

Androgen receptor pathway inhibitors (ARPIs), including abiraterone acetate, enzalutamide, apalutamide, and darolutamide, have become widely used in the treatment of metastatic hormone-sensitive prostate cancer (mHSPC) and metastatic castration-resistant prostate cancer (mCRPC). Several clinical and molecular factors are associated with poor outcomes in patients receiving ARPIs, including high Gleason score, presence of liver metastases, high disease volume, *de novo* metastatic presentation, elevated baseline prostate-specific antigen (PSA), low hemoglobin levels, elevated alkaline phosphatase levels, and AR-V7 positivity (16-25). Although several retrospective studies showed that presence of IDC-P was associated with shorter CRPC-free survival, PSA progression-free survival (PSA-PFS) and OS in patients who treated with ARPIs, data on the prognostic impact of uncommon histological subtypes in patients treated with ARPIs is limited (26-28). This study aimed to evaluate the prognostic impact of IDC-P in patients with metastatic prostate cancer who were treated with enzalutamide or abiraterone acetate.

Materials and Methods

We conducted a retrospective single-center cohort study in the Department of Medical Oncology at Ankara University. The study adhered to the principles outlined in the Declaration of Helsinki and received ethical approval from the Ankara University Faculty of Medicine Ethics Committee (decision no: İ06-428-24, date: 13.06.2024). The study included patients with metastatic prostate adenocarcinoma who received abiraterone acetate or enzalutamide from January 1, 2014, to December 2024. Patients who received androgen deprivation therapy (ADT) or a single line of docetaxel treatment were eligible for the study. Patients who received more than one line of docetaxel or who received treatment other than ADT or docetaxel prior to ARPI treatment were excluded from the study. We excluded patients who received triplet therapy, which included ADT, an ARPI, and docetaxel. Patients whose pathology results were unavailable or who were diagnosed based solely on non-prostatic tissue samples were excluded from the study. Additionally, patients with incomplete data that prevented us from conducting survival analyses for secondary malignancy and for pure neuroendocrine pathology were excluded from the study.

Patient demographics, Eastern Cooperative Oncology Group (ECOG) performance status, laboratory findings, and timelines for diagnosis, treatment, progression, and death were retrospectively extracted. High volume disease was defined as the presence of visceral metastases or ≥4 bone lesions with ≥1 beyond the vertebral bodies and pelvis. The primary outcome of the study was OS. OS was defined as the time from the start of the ARPI (abiraterone acetate or enzalutamide) to death. Secondary outcomes were PSA-PFS, radiologic PFS (rPFS), and PSA50 response rate. PSA-PFS was defined as the interval between the initiation of ARPI (abiraterone acetate or enzalutamide) and PSA progression or death. PSA progression was characterized by a ≥25% increase in PSA levels, reaching at least 2 ng/mL, and confirmed by a subsequent measurement taken at least 3 weeks later, in accordance with the PCWG3 criteria (29). rPFS was defined as the interval between the initiation of the ARPI (abiraterone acetate or enzalutamide) and the time at radiologic progression according to PCWG3 criteria or death (29). PSA50 response rate was defined as the proportion of participants with a PSA reduction of 50% or more from baseline.

Statistical Analysis

All statistical analyses were conducted using IBM SPSS Statistics version 24.0. Continuous variables were presented as medians with interquartile ranges (IQR), while categorical variables were expressed as frequencies and percentages. Comparisons between categorical variables were performed using the chi-square test. For continuous variables, the Mann-Whitney U test or Student's t-test was applied, depending on the distribution of the data. Survival outcomes were estimated using the Kaplan-Meier method. Variables with a p-value ≤0.10 in univariate analyses were included in multivariate models. Cox proportional hazards regression (backward likelihood ratio method) was used for multivariable analysis to estimate hazard ratios (HR) with 95% confidence intervals (CI). All p-values were two-sided, and values <0.05 were considered statistically significant.

Results

A total of 254 patients with metastatic prostate cancer who were treated with abiraterone acetate or enzalutamide were screened. Ninety-four men who met the inclusion criteria, whose median age was 68.9 years (IQR=12.8), were included in the study. Of these patients, 79 (84%) have ECOG 0 or 1 performance status. A total of 69 patients (73.4%) had a Gleason grade group >7, and IDC-P was identified in 19 patients (20.2%). While 39 patients (41.5%) were treated with abiraterone acetate, 55 patients (58.5%) received enzalutamide. ARPIs were administered for mHSPC in 30 patients (31.9%) and for mCRPC in 64 patients (68.1%). The most common metastatic site was the bone (85.1%), followed by the lymph node (64.9%) and the lung (16%). All baseline characteristics are shown in Table 1. Patients with and without IDC-P had similar characteristics overall, except for the disease setting at initiation of ARPI therapy and the presence of bone and lung metastases (Table 1).

The median follow-up time was 54.14 months (95% CI 43.30-64.99). Median OS was 49.18 months (95% CI 36.39-61.96). Median OS was significantly shorter in patients with IDC-P [35.38 months (95% CI 19.58-51.19)] compared to patients without IDC-P [55.59 months (95% CI 45.05-66.13)] (p=0.011) (Figure 1A). In the mHSPC cohort, the median OS was not reached in patients without IDC-P, whereas it was 35.48 months (95% CI 12.31-58.65) in those with IDC-P (p=0.073) (Figure 1B). In the mCRPC cohort, the median OS was 49.93 months (95% CI 37.78-62.09) in patients without IDC-P and 35.38 months (95% CI 10.37-60.40) in patients with IDC-P (p=0.035) (Figure 1C). In the mCRPC cohort, among patients previously treated with docetaxel, median OS was 25.13 months (95% CI 3.23-47.03) in those with IDC-P versus 45.96 months (95% CI 33.41-58.52) in those without IDC-P (p=0.035). Multivariate Cox regression analysis showed that the presence of IDC-P was an independent predictor of poor OS (HR 3.16, 95% CI 1.56-6.41; p=0.001) after adjusting for confounding factors, such as ECOG performance status, Gleason grade group, presence of high grade prostatic intraepithelial neoplasia (HGPIN), type of ARPI, and disease volume (Table 2).

Median PSA-PFS was 28.42 months (95% CI 22.28-34.56). The median PSA-PFS was 15.87 months (95% CI 6.55-25.19) for patients with IDC-P and 31.11 months (95% CI 23.43-40.77) for patients without IDC-P (p=0.020) (Figure 2A). In the mHSPC cohort, the median PSA-PFS was not reached in patients without IDC-P, whereas it was 18.33 months (95% CI 6.71-29.96) in those with IDC-P (p=0.073) (Figure 2B). In the mCRPC cohort, the median PSA-PFS was 28.42 months (95% CI 21.32-35.51) in patients without IDC-P and 15.87 months (95% CI 1.48-30.27) in patients with IDC-P (p=0.011) (Figure 2C). In the mCRPC cohort, among patients previously treated with docetaxel, the median PSA-PFS was 28.38 months (95% CI 22.28-34.49) in patients without IDC-P and 15.87 months (95% CI 0.07-31.66) in patients with IDC-P (p=0.032). Multivariate Cox regression analysis showed that the presence of IDC-P was an independent predictor of poor PSA-PFS (HR 2.14, 95% CI 1.15-3.99; p=0.017) after adjusting for confounding factors, such as Gleason grade group, presence of HGPIN, type of ARPI, and disease volume (Table 3).

The median rPFS for the entire population was 33.18 months (95% CI 27.57-38.79). Although patients with IDC-P had numerically longer rPFS, the difference was not statistically significant [23.62 months (95% CI 13.53-33.71) for patients with IDC-P versus 34.20 months (95% CI 26.37-42.03) for those without IDC-P; p=0.091] (Figure 3A). In the mHSPC cohort, the median rPFS was not reached in patients without IDC-P, whereas median rPFS was 23.62 months (95% CI, NE-NE) in those with IDC-P (p=0.395) (Figure 3B). In the mCRPC cohort, the median rPFS was 33.18 months (95% CI 27.21-39.15) in patients without IDC-P and 21.49 months (95% CI 3.63-39.34) in patients with IDC-P (p=0.030) (Figure 3C). In the mCRPC cohort, among patients previously treated with

Table 1. General characteristic of the patients

		All patients (n=94)	IDC-P (-) (n=75)	IDC-P (+) (n=19)	p
Age	**Median (IQR)**	68.96 (12.8)	68.89 (14.2)	68.06 (7.5)	0.204
	<65	33 (35.1)	24 (32)	9 (47.4)	0.282
	≥65	61 (64.9)	51 (68)	10 (52.6)	
ECOG performance status	**0-1**	79 (84)	65 (86.7)	14 (73.7)	0.206
	2	12 (12.8)	8 (10.7)	4 (21)	
	Unknown	3 (3.2)	2 (2.7)	1 (5.3)	
Grade group	**≤7**	25 (26.6)	23 (30.7)	2 (10.5)	0.089
	>7	69 (73.4)	52 (69.3)	17 (89.5)	
Cribriform pattern		4 (4.3)	3 (4)	1 (5.3)	0.807
HGPIN		13 (13.8)	12 (16)	1 (5.3)	0.226
Neuroendocrine differentiation		3 (3.2)	1 (1.3)	2 (10.5)	0.042
***De novo* metastatic disease**		64 (68.1)	49 (65.3)	15 (78.9)	0.242
Disease setting at initiation of ARPIs	**mHSPC**	30 (31.9)	20 (26.7)	10 (52.6)	**0.030**
	mCRPC	64 (68.1)	55 (73.3)	9 (47.4)	
Prior treatment for mPCa (among mCRPC patients)	**ADT**	16 (25)	15 (27.3)	1 (11.1)	0.229
	ADT + docetaxel	48 (75)	40 (72.7)	8 (88.9)	
ARPI type	**Abiraterone**	39 (41.5)	34 (45.3)	5 (26.3)	0.193
	Enzalutamide	55 (58.5)	41 (54.7)	14 (73.7)	
Bone metastasis		80 (85.1)	61 (81.3)	19 (100)	**0.041**
≤4		18 (19.1)	14 (18.7)	4 (21.1)	0.099
5-10		13 (13.8)	8 (10.7)	5 (26.3)	
>10		49 (52.1)	39 (52)	10 (52.6)	
Lymph node metastasis		61 (64.9)	48 (64)	13 (68.4)	0.793
Lung metastasis		15 (16)	15 (20)	0	**0.033**
Liver metastasis		5 (5.3)	5 (6.7)	0	0.247
Disease volume	**Low**	32 (34)	25 (33.3)	7 (36.8)	0.791
	High	62 (66)	50 (66.7)	12 (63.2)	
Bone modifying agent		57 (60.6)	45 (60)	12 (63.2)	0.801

ADT: Androgen deprivation treatment, ARPI: Androgen receptor pathway inhibitor, ECOG: Eastern Cooperative Oncology Group, HGPIN: High grade prostatic intraepithelial neoplasia, IDC-P: Intraductal carcinoma of prostate, IQR: Interquartile range, mCRPC: Metastatic castration-resistant prostate cancer, mHSPC: Metastatic hormone-sensitive prostate cancer, mPCa: Metastatic prostate cancer

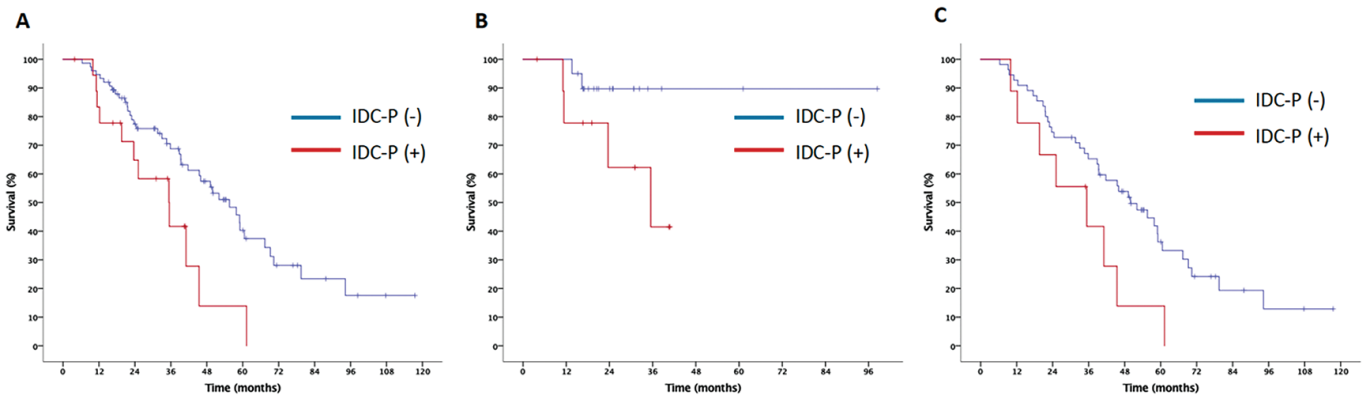

Figure 1. Kaplan-Meier curves for overall survival in the entire cohort (A), mHSPC subgroup (B) and mCRPC subgroup (C)

IDC-P: Intraductal carcinoma of the prostate, mHSPC: Metastatic hormone-sensitive prostate cancer, mCRPC: Metastatic castration-resistant prostate cancer

Table 2. Univariate and multivariate analysis for predictors of overall survival

Variable		Univariate HR (95% CI)	p	Multivariate* HR (95% CI)	p	Multivariate** HR (95% CI)	p
Age	<65	1		-		-	
	≥65	0.83 (0.47-1.46)	0.518	-	-	-	-
ECOG-PS	0-1	1		1		1	
	2	2.41 (1.16-5.00)	0.018	2.05 (0.89-4.71)	0.089	2.26 (1.02-5.00)	0.044
Grade group	≤7	1		1		-	
	>7	1.97 (1.01-3.85)	0.047	1.20 (0.56-2.58)	0.643	-	-
IDC-P	No	1		1		1	
	Yes	2.33 (1.19-4.57)	0.014	2.78 (1.34-5.75)	0.006	3.16 (1.56-6.41)	0.001
HGPIN	No	1		1		-	
	Yes	0.37 (0.13-1.03)	0.057	0.46 (0.13-1.62)	0.227	-	-
De novo metastasis	No	1		-		-	
	Yes	0.85 (0.48-1.51)	0.578	-	-	-	-
Disease setting at initiation of ARPIs	mHSPC	1		-		-	
	mCRPC	1.78 (0.75-4.23)	0.140	-	-	-	-
ARPI	Abiraterone	1		1		1	
	Enzalutamide	0.58 (0.33-0.99)	0.050	0.58 (0.31-1.09)	0.092	0.05 (0.27-0.91)	0.023
Prior treatment	ADT	1		-		-	
	ADT + docetaxel	1.82 (0.84-3.94)	0.128	-	-	-	-
Bone metastasis	No	1		-		-	
	Yes	1.74 (0.69-4.40)	0.238	-	-	-	-
Lymph node metastasis	No	1		-		-	
	Yes	1.63 (0.91-2.94)	0.101	-	-	-	-
Lung metastasis	No	1		-		-	
	Yes	1.22 (0.64-2.33)	0.551	-	-	-	-
Liver metastasis	No	1		-		-	
	Yes	0.72 (0.22-2.33)	0.589	-	-	-	-
Disease volume	Low	1		1		1	
	High	2.47 (1.20-5.07)	0.014	2.42 (1.13-5.19)	0.023	2.44 (1.14-5.19)	0.023

*: First step in cox regression analysis, **: Final step in cox regression analysis, ADT: Androgen deprivation treatment, ARPI: Androgen receptor pathway inhibitor, CI: Confidence interval, ECOG: Eastern Cooperative Oncology Group, HGPIN: High grade prostatic intraepithelial neoplasia, HR: Hazard ratio, IDC-P: Intraductal carcinoma of prostate, mCRPC: Metastatic castration-resistant prostate cancer, mHSPC: Metastatic hormone-sensitive prostate cancer, PS: Performance status

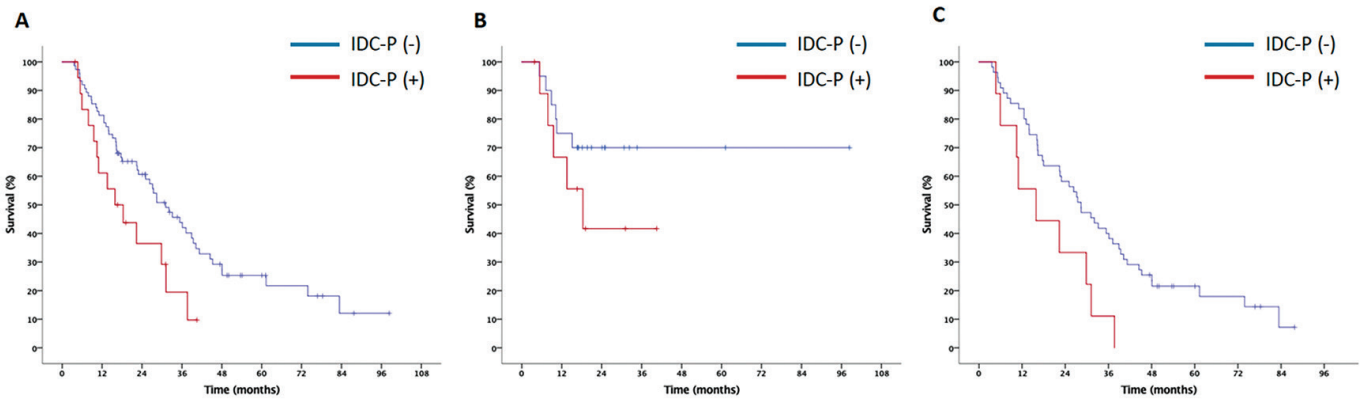

Figure 2. Kaplan-Meier curves for PSA-PFS in the entire cohort (A), mHSPC subgroup (B) and mCRPC subgroup (C)

IDC-P: Intraductal carcinoma of the prostate, mHSPC: Metastatic hormone-sensitive prostate cancer, mCRPC: Metastatic castration-resistant prostate cancer, PSA-PFS: Prostate specific antigen-progression free survival

Table 3. Univariate and multivariate analysis for predictors of PSA progression free survival

Variable		Univariate HR (95% CI)	p	Multivariate* HR (95% CI)	p	Multivariate** HR (95% CI)	p
Age	<65	1		-		-	
	≥65	0.95 (0.56-1.59)	0.834	-	-	-	-
ECOG-PS	0-1	1		-		-	
	2	1.72 (0.87-3.41)	0.118	-	-	-	-
Grade group	≤7	1		1		-	
	>7	1.28 (1.03-1.59)	0.028	1.10 (0.61-2.01)	0.746	-	-
IDC-P	No	1		1		1	
	Yes	2.04 (1.10-3.75)	0.023	2.09 (1.11-3.95)	0.023	2.14 (1.15-3.99)	0.017
HGPIN	No	1		1		1	
	Yes	0.27 (0.09-0.75)	0.012	0.35 (0.12-1.02)	0.054	0.34 (0.12-0.96)	0.042
De novo metastasis	No	1		-		-	
	Yes	0.71 (0.42-1.18)	0.184	-	-	-	-
Disease setting at initiation of ARPIs	mHSPC	1		-		-	
	mCRPC	1.52 (0.79-2.93)	0.212	-	-	-	-
ARPI	Abiraterone	1		1		1	
	Enzalutamide	0.59 (0.36-0.96)	0.035	0.66 (0.39-1.08)	0.097	0.65 (0.40-1.08)	0.095
Prior treatment	ADT	1		-		-	
	ADT + docetaxel	0.89 (0.48-1.68)	0.737	-	-	-	-
Bone metastasis	No	1		-		-	
	Yes	1.78 (0.81-3.91)	0.150	-	-	-	-
Lymph node metastasis	No	1		-		-	
	Yes	1.51 (0.89-2.58)	0.128	-	-	-	-
Lung metastasis	No	1		-		-	
	Yes	1.18 (0.64-2.19)	0.590	-	-	-	-
Liver metastasis	No	1		-		-	
	Yes	0.97 (0.35-2.68)	0.949	-	-	-	-
Disease volume	Low	1		1		1	
	High	1.79 (1.06-3.15)	0.044	1.94 (1.09-3.47)	0.025	1.96 (1.10-3.49)	0.022

*: First step in cox regression analysis, **: Final step in cox regression analysis, ADT: Androgen deprivation treatment, ARPI: Androgen receptor pathway inhibitor, CI: Confidence interval, ECOG: Eastern Cooperative Oncology Group, HGPIN: High grade prostatic intraepithelial neoplasia, HR: Hazard ratio, IDC-P: Intraductal carcinoma of prostate, mCRPC: Metastatic castration-resistant prostate cancer, mHSPC: Metastatic hormone-sensitive prostate cancer, PS: Performance status, PSA: Prostate specific antigen

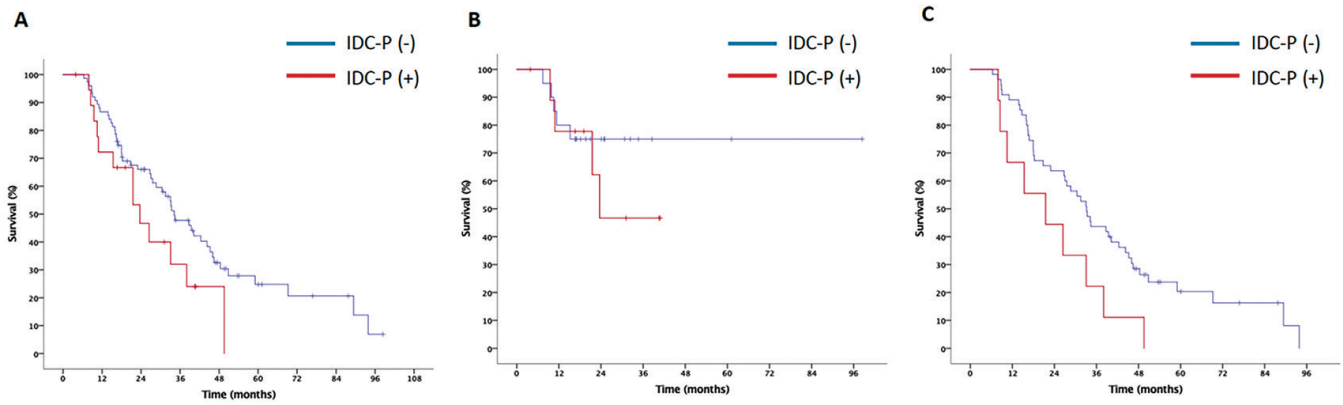

Figure 3. Kaplan-Meier curves for rPFS in the entire cohort (A), mHSPC subgroup (B) and mCRPC subgroup (C)

IDC-P: Intraductal carcinoma of the prostate, mHSPC: Metastatic hormone-sensitive prostate cancer, mCRPC: Metastatic castration-resistant prostate cancer, rPFS: Radiologic progression free survival

Table 4. Univariate and multivariate analysis for predictors of radiologic progression free survival

Variable		Univariate HR (95% CI)	p	Multivariate* HR (95% CI)	p	Multivariate** HR (95% CI)	p
Age	<65	1		-		-	-
	≥65	0.77 (0.46-1.29)	0.316	-		-	-
ECOG-PS	0-1	1		1		-	
	2	1.79 (0.90-3.54)	0.097	1.31 (0.63-2.72)	0.468	-	-
Grade group	≤7	1		1		-	
	>7	1.85 (1.02-3.37)	0.044	1.16 (0.58-2.30)	0.673	-	-
IDC-P	No	1		1		-	
	Yes	1.70 (0.91-3.18)	0.095	1.92 (0.93-3.96)	0.078	-	-
HGPIN	No	1		1		1	
	Yes	0.27 (0.10-0.74)	0.011	0.29 (0.08-1.01)	0.051	0.21 (0.06-0.68)	0.010
De novo metastasis	No	1		-		-	
	Yes	0.71 (0.42-1.19)	0.199	-	-	-	-
Disease setting at initiation of ARPIs	mHSPC	1		1		-	
	mCRPC	1.96 (0.96-3.99)	0.066	1.50 (0.68-3.31)	0.314	-	-
ARPI	Abiraterone	1		-		-	
	Enzalutamide	0.72 (0.43-1.18)	0.192	-	-	-	-
Prior treatment	ADT	1		-		-	
	ADT + docetaxel	1.23 (0.63-2.41)	0.544	-	-	-	-
Bone metastasis	No	1		-		-	
	Yes	1.46 (0.67-3.22)	0.342	-	-	-	-
Lymph node metastasis	No	1		-		-	
	Yes	1.23 (0.73-2.07)	0.444	-	-	-	-
Lung metastasis	No	1		-		-	
	Yes	1.59 (0.87-2.89)	0.132	-	-	-	-
Liver metastasis	No	1		1		-	
	Yes	2.23 (0.87-5.69)	0.094	1.74 (0.64-4.75)	0.227	-	-
Disease volume	Low	1		1		1	
	High	2.19 (1.21-3.97)	0.010	2.22 (1.12-4.38)	0.022	2.44 (1.31-4.55)	0.005

*: First step in cox regression analysis, **: Final step in cox regression analysis, ADT: Androgen deprivation treatment, ARPI: Androgen receptor pathway inhibitor, CI: Confidence interval, ECOG: Eastern Cooperative Oncology Group, HGPIN: High grade prostatic intraepithelial neoplasia, HR: Hazard ratio, IDC-P: Intraductal carcinoma of prostate, mCRPC: Metastatic castration-resistant prostate cancer, mHSPC: Metastatic hormone-sensitive prostate cancer, PS: Performance status

docetaxel, the median rPFS was 33.08 months (95% CI 28.54-37.49) for patients without IDC-P and 21.49 months (95% CI 6.14-36.83) for patients with IDC-P (p=0.086). Multivariate Cox regression analysis for rPFS is presented in Table 4. The PSA50 response rate was assessed in 93 patients. The PSA50 response was 43% for the entire population. There was no difference in PSA50 response rate between groups (50% for patients with IDC-P and 41.3% for patients without IDC-P; p=0.599).

Discussion

IDC-P is acknowledged as an adverse prognostic factor in nonmetastatic prostate cancer (14,15,30,31). However, the impact of IDC-P on the prognosis of metastatic prostate cancer is limited. Our findings suggest that the presence of IDC-P on pathological examination is a poor prognostic factor for patients with metastatic prostate cancer who are treated with enzalutamide or abiraterone acetate. OS (35.38-55.59) and PSA-PFS (15.87-31.11 months) were significantly shorter in patients with IDC-P.

While conventional acinar adenocarcinoma constitutes the vast majority of prostate cancer cases (95%), approximately 5% exhibit unconventional histological subtypes (32). Considering the high global incidence of prostate cancer, the second most common malignancy in men, this minority still represents a clinically significant number of patients (33). New entities, including IDC-P, were introduced in the 2016 WHO classification (3). Cribriform growth pattern and IDC-P are now recommended to be routinely reported in prostate cancer pathology (34,35). Although the recognition of unconventional histologies in prostate cancer has markedly increased over the past decade, substantial inter-center variability in pathological reporting suggests a lack of standardization, and prostate biopsy procedures likely underestimate the true incidence of these unconventional histological subtypes (31,36).

A retrospective study that evaluated the prognostic impact of ductal features in patients with *de novo* metastatic prostate carcinoma who were treated only with ADT found no significant difference in outcomes between patients with ductal adenocarcinoma and those with pure acinar adenocarcinoma. However, the presence of IDC-P was identified as an independent adverse prognostic factor for both CRPC-free survival (HR 1.84, 95% CI 1.48-2.30) and OS (HR 1.56; 95% CI 1.05-2.31) (37). Several additional studies showed that IDC-P was associated with shorter castration-resistant prostate cancer-free survival and OS (26-28,38,39). In a retrospective study including patients with mCRPC, IDC-P positivity was associated with a poorer PSA response to docetaxel than to abiraterone acetate (21.7% vs. 52.4%). Median PSA-PFS was also significantly longer with abiraterone acetate in patients with IDC-P (13.5 vs. 6.0 months; p=0.012), whereas no such difference was seen in patients without IDC-P. Although not statistically significant, a trend toward longer OS with abiraterone acetate was observed in the IDC-P positive group (26). In another study of mCRPC patients treated with abiraterone acetate or enzalutamide, the presence of IDC-P was associated with a significantly shorter OS (57.9 vs. 38.0 months). Although PFS was numerically lower in patients with IDC-P (10.6 vs. 6.2 months), the difference did not reach statistical significance (28). These findings are largely consistent with our results, although the median PFS and OS in our study were longer, likely due to the inclusion of both mHSPC and mCRPC patients. Not only is the presence of IDC-P important for prognosis, but also its proportion and histological pattern may have prognostic significance (27). Enzalutamide use was associated with longer OS compared to abiraterone acetate. No head-to-head clinical trials have compared enzalutamide and abiraterone acetate. Although clinical trials of abiraterone acetate and enzalutamide differed in inclusion criteria and excluded patients with certain comorbidities, several meta-analyses and retrospective studies have shown enzalutamide to provide superior rPFS, PSA-PFS, and PSA response rates compared to abiraterone acetate (40-45). The superior efficacy of enzalutamide may relate to its distinct mechanism of action. Enzalutamide blocks downstream AR signaling, including nuclear translocation and transcription, and may thereby overcome resistance due to AR overactivity or mutation.

Study Limitations

This study has several limitations. First, as a retrospective analysis, it is subject to inherent biases, including selection bias, unmeasured confounding, and missing data, all of which may have influenced the outcomes. Second, the relatively small sample size, especially for patients with mHSPC, may have limited the power to detect a difference in rPFS. Nevertheless, the cohort remains one of the largest evaluating the prognostic impact of IDC-P in patients treated with ARPIs. In addition, combining mHSPC and mCRPC patients within a single survival model constitutes a methodological limitation, as differing baseline hazards between these disease settings may have influenced the observed outcomes. Although the study was conducted at a single institution, pathological evaluations were performed by different pathologists. Thus, inter-observer variability remains a potential source of heterogeneity. In addition, the patient population and prior treatments were heterogeneous, which may have further influenced the outcomes. Lastly, the relatively long inclusion period may have introduced variability in diagnostic awareness and reporting standards over time.

Conclusion

This study demonstrates that the presence of IDC-P is a poor prognostic factor for PSA-PFS and OS in patients with metastatic prostate cancer treated with abiraterone acetate or enzalutamide. Although there is growing evidence supporting the aggressive behavior of IDC-P, nearly all available data are retrospective. Therefore, prospective studies with larger cohorts are needed to establish the reliability and clinical applicability of these findings. Despite growing molecular insights into IDC-P, much of the data derive from retrospective histological analyses of prostate cancer cases. Comprehensive studies are required to better elucidate the behavior of these unconventional prostate cancer subtypes.

Ethics

Ethics Committee Approval: The study adhered to the principles outlined in the Declaration of Helsinki and received ethical approval from the Ankara University Faculty of Medicine Ethics Committee (decision no: İ06-428-24, date: 13.06.2024).

Informed Consent: Retrospective study.

Acknowledgements

Publication: The results of the study were not published in full or in part in form of abstracts.

Contribution: There is not any contributors who may not be listed as authors.

Footnotes

Authorship Contributions

Surgical and Medical Practices: H.B., S.C.Y., E.Y., Y.Ü., Concept: H.B., Design: H.B., E.Y., Y.Ü., Data Collection or Processing: H.B., S.C.Y., Analysis or Interpretation: H.B., Literature Search: H.B., Writing: H.B., S.C.Y., E.Y., Y.Ü.

Conflict of Interest: No conflict of interest was declared by the authors.

Financial Disclosure: The authors declared that this study received no financial support.

References

1. Birindelli G, Drobnjakovic M, Morath V, et al. In silico study on radiobiological efficacy of Ac-225 and Lu-177 for PSMA-guided radiotherapy. Annu Int Conf IEEE Eng Med Biol Soc. 2021;2021:4497-4500.
2. McNeal JE, Yemoto CE. Spread of adenocarcinoma within prostatic ducts and acini. Morphologic and clinical correlations. Am J Surg Pathol. 1996;20:802-814.
3. Humphrey PA, Moch H, Cubilla AL, Ulbright TM, Reuter VE. The 2016 WHO classification of tumours of the urinary system and male genital organs-part B: prostate and bladder tumours. Eur Urol. 2016;70:106-119.
4. Kato M, Hirakawa A, Kobayashi Y Ms, et al. The influence of the presence of intraductal carcinoma of the prostate on the grade group system's prognostic performance. Prostate. 2019;79:1065-1070.
5. Porter LH, Lawrence MG, Ilic D, et al. Systematic review links the prevalence of intraductal carcinoma of the prostate to prostate cancer risk categories. Eur Urol. 2017;72:492-495.
6. Netto GJ, Amin MB, Berney DM, et al. The 2022 World Health Organization classification of tumors of the urinary system and male genital organs-part B: prostate and urinary tract tumors. Eur Urol. 2022;82:469-482.
7. Watts K, Li J, Magi-Galluzzi C, Zhou M. Incidence and clinicopathological characteristics of intraductal carcinoma detected in prostate biopsies: a prospective cohort study. Histopathology. 2013;63:574-579.
8. Cohen RJ, Chan WC, Edgar SG, et al. Prediction of pathological stage and clinical outcome in prostate cancer: an improved pre-operative model incorporating biopsy-determined intraductal carcinoma. Br J Urol. 1998;81:413-418.
9. Wilcox G, Soh S, Chakraborty S, Scardino PT, Wheeler TM. Patterns of high-grade prostatic intraepithelial neoplasia associated with clinically aggressive prostate cancer. Hum Pathol. 1998;29:1119-1123.
10. Ekmekci S, Talu ECK, Kısa E, Küçük Ü. The relationship of morphological tumor heterogeneity with lymph node metastasis in prostatic adenocarcinomas. İzmir Tıp Fak Derg. 2023;2:122-128.
11. Bernhardt M, Kristiansen G. Molecular alterations in intraductal carcinoma of the prostate. Cancers (Basel). 2023;15:5512.
12. Kang M, Lee H, Byeon SJ, Kwon GY, Jeon SS. Genomic features and clinical implications of intraductal carcinoma of the prostate. Int J Mol Sci. 2021;22:13125.
13. Zhu S, Xu N, Zeng H. Molecular complexity of intraductal carcinoma of the prostate. Cancer Med. 2024;13:e6939.
14. Dinerman BF, Khani F, Golan R, et al. Population-based study of the incidence and survival for intraductal carcinoma of the prostate. Urol Oncol. 2017;35:673.e9-673.e14.
15. Van der Kwast T, Al Daoud N, Collette L, et al. Biopsy diagnosis of intraductal carcinoma is prognostic in intermediate and high risk prostate cancer patients treated by radiotherapy. Eur J Cancer. 2012;48:1318-1325.
16. Halabi S, Kelly WK, Ma H, et al. Meta-analysis evaluating the impact of site of metastasis on overall survival in men with castration-resistant prostate cancer. J Clin Oncol. 2016;34:1652-1659.
17. Hamid AA, Thomas H, Martin A, et al. 1618P clinical prognostic factors within the high volume subgroup of metastatic hormone sensitive prostate cancer (mHSPC) in ENZAMET (ANZUP 1304). Ann Oncol. 2024;35:977-978.
18. Sweeney CJ, Martin AJ, Stockler MR, et al.; ENZAMET trial investigators and Australian and New Zealand Urogenital and Prostate Cancer Trials Group. Testosterone suppression plus enzalutamide versus testosterone suppression plus standard antiandrogen therapy for metastatic hormone-sensitive prostate cancer (ENZAMET): an international, open-label, randomised, phase 3 trial. Lancet Oncol. 2023;24:323-334.
19. Choi SY, Ryu J, You D, et al. Prognostic factors of oncologic outcomes in metastatic chemotherapy-naïve castration-resistant prostate cancer treated with enzalutamide in actual clinical practice in East Asia. Urol Oncol. 2018;36:401.e11-401.e18.
20. Armstrong AJ, Lin P, Higano CS, et al. Development and validation of a prognostic model for overall survival in chemotherapy-naïve men with metastatic castration-resistant prostate cancer. Ann Oncol. 2018;29:2200-2207.
21. Chi KN, Kheoh T, Ryan CJ, et al. A prognostic index model for predicting overall survival in patients with metastatic castration-resistant prostate cancer treated with abiraterone acetate after docetaxel. Ann Oncol. 2016;27:454-460.
22. Armstrong AJ, Lin P, Tombal B, et al. Five-year survival prediction and safety outcomes with enzalutamide in men with chemotherapy-naïve metastatic castration-resistant prostate cancer from the PREVAIL trial. Eur Urol. 2020;78:347-357.
23. Kyriakopoulos CE, Chen YH, Carducci MA, et al. Chemohormonal therapy in metastatic hormone-sensitive prostate cancer: long-term survival analysis of the randomized phase III E3805 CHAARTED trial. J Clin Oncol. 2018;36:1080-1087.
24. Antonarakis ES, Lu C, Wang H, et al. AR-V7 and resistance to enzalutamide and abiraterone in prostate cancer. N Engl J Med. 2014;371:1028-1038.
25. Akay SU, Seyyar M. Radiotherapy for oligometastatic prostate cancer. Bull Urooncol. 2024;23:63-67
26. Zhao J, Shen P, Sun G, et al. The prognostic implication of intraductal carcinoma of the prostate in metastatic castration-resistant prostate cancer and its potential predictive value in those treated with docetaxel or abiraterone as first-line therapy. Oncotarget. 2017;8:55374-55383.
27. Zhao J, Liu J, Sun G, et al.; Collaborators. The prognostic value of the proportion and architectural patterns of intraductal carcinoma of the prostate in patients with *de novo* metastatic prostate cancer. J Urol. 2019;201:759-768.
28. Abascal-Junquera JM, Fumadó-Ciutat L, Gasa-Galmes B, et al. Concomitant intraductal carcinoma of the prostate and response to hormonal therapy in metastatic prostate carcinoma. Actas Urol Esp (Engl Ed). 2021;45:455-460. English, Spanish.

29. Scher HI, Morris MJ, Stadler WM, et al.; Prostate Cancer Clinical Trials Working Group 3. Trial design and objectives for castration-resistant prostate cancer: updated recommendations from the prostate cancer clinical trials working group 3. J Clin Oncol. 2016;34:1402-1418.
30. Kim A, Kwon T, You D, et al. Clinicopathological features of prostate ductal carcinoma: matching analysis and comparison with prostate acinar carcinoma. J Korean Med Sci. 2015;30:385-389.
31. Pahouja G, Patel HD, Desai S, et al. The rising incidence of ductal adenocarcinoma and intraductal carcinoma of the prostate: diagnostic accuracy of biopsy, MRI-visibility, and outcomes. Urol Oncol. 2023;41:48.e11-48.e18.
32. WHO Classification of Tumours Editorial Board. Urinary and male genital tumours. WHO Classification of Tumours. 5th ed. Vol. 8. Lyon: International Agency for Research on Cancer; 2022.
33. Bray F, Laversanne M, Sung H, et al. Global cancer statistics 2022: GLOBOCAN estimates of incidence and mortality worldwide for 36 cancers in 185 countries. CA Cancer J Clin. 2024;74:229-263.
34. Epstein JI, Amin MB, Fine SW, et al. The 2019 Genitourinary Pathology Society (GUPS) white paper on contemporary grading of prostate cancer. Arch Pathol Lab Med. 2021;145:461-493.
35. van Leenders GJLH, van der Kwast TH, Iczkowski KA. The 2019 International Society of Urological pathology consensus conference on prostate cancer grading. Eur Urol. 2021;79:707-709.
36. Marra G, van Leenders GJLH, David G, et al. Assessment of the reporting and incidence of prostate cancer unconventional histologies in tertiary referral institutions: an under-reported but exploding phenomenon? Eur Urol Oncol. 2025;8:875-878.
37. Wu T, Zhao J, Liu Z, et al. Does ductal adenocarcinoma of the prostate (DA) have any prognostic impact on patients with *de novo* metastatic prostate cancer? Prostate. 2019;79:1673-1682.
38. Zhao T, Liao B, Yao J, et al. Is there any prognostic impact of intraductal carcinoma of prostate in initial diagnosed aggressively metastatic prostate cancer?. Prostate. 2015;75:225-232.
39. Chen Z, Chen N, Shen P, et al. The presence and clinical implication of intraductal carcinoma of prostate in metastatic castration resistant prostate cancer. Prostate. 2015;75:1247-1254.
40. Fang M, Nakazawa M, Antonarakis ES, Li C. Efficacy of abiraterone and enzalutamide in pre- and postdocetaxel castration-resistant prostate cancer: a trial-level meta-analysis. Prostate Cancer. 2017;2017:8560827.
41. Wei Z, Chen C, Li B, Li Y, Gu H. Efficacy and safety of abiraterone acetate and enzalutamide for the treatment of metastatic castration-resistant prostate cancer: a systematic review and meta-analysis. Front Oncol. 2021;11:732599.
42. McCool R, Fleetwood K, Glanville J, Arber M, Goodall H, Naidoo S. Systematic review and network meta-analysis of treatments for chemotherapy-naive patients with asymptomatic/mildly symptomatic metastatic castration-resistant prostate cancer. Value Health. 2018;21:1259-1268.
43. La J, Wang L, Corrigan JK, et al. Abiraterone or enzalutamide for patients with metastatic castration-resistant prostate cancer. JAMA Netw Open. 2024;7:e2428444.
44. Horváth A, Blasszauer C, Komka I, et al. Real-world overall survival comparison of enzalutamide and abiraterone in first- and second-line setting of metastatic castration-resistant prostate cancer. Prostate. 2025;85:1151-1154.
45. George DJ, Ramaswamy K, Yang H, et al. Real-world overall survival with abiraterone acetate versus enzalutamide in chemotherapy-naïve patients with metastatic castration-resistant prostate cancer. Prostate Cancer Prostatic Dis. 2024;27:756-764.

Case Report

DOI: 10.4274/uob.galenos.2025.2025.2.5

Bull Urooncol 2026;25(1):27-30

Kidney Metastasis of Small Cell Lung Cancer Under Immunotherapy: Case Report

Günal Özgür[1], Murat Kars[1], İhsan Turan Ceran[2], Muhammed Hasan Toper[2], Abdussamet Çelebi[3], Yusuf Şenoğlu[4]

[1]*Marmara University Pendik Training and Research Hospital, Department of Urology, İstanbul, Türkiye*
[2]*Marmara University Pendik Training and Research Hospital, Department of Pathology, İstanbul, Türkiye*
[3]*Marmara University Pendik Training and Research Hospital, Department of Oncology, İstanbul, Türkiye*
[4]*Marmara University Faculty of Medicine, Department of Urology, İstanbul, Türkiye*

Abstract

Renal metastasis from small cell lung cancer (SCLC) is highly uncommon. A 60-year-old woman received chemotherapy and radiotherapy for metastatic SCLC. The patient remained in remission for 18 months on adjuvant atezolizumab. Follow-up radiological staging revealed a solitary renal mass. Then she underwent laparoscopic nephrectomy. The pathological examination confirmed SCLC metastasis. This case report suggested that isolated renal metastasis can be seen in patients with SCLC even under maintenance immunotherapy.
Keywords: Kidney tumors, lung cancer, metastases, nephrectomy, small cell carcinoma

Introduction

The most common tumor types causing metastasis to the kidney are lung (43.7%), colorectal (10.6%), head and neck (6%), breast (5.3%), soft tissue (5.3%), and thyroid (5.3%) (1,2). Although renal metastasis has been reported in all types of lung cancers, squamous cell carcinoma (57.6%), adenocarcinoma (28.8%), and small cell lung carcinoma (SCLC) (5.1%) are frequent histological subtypes (3). On the other hand, renal metastasis of SCLC is extremely rare. Based on our review of the literature, this appears to be the first report demonstrating RM of SCLC under maintenance immunotherapy.

Case Reports

A 58-year-old woman with diabetes and hypertension was found to have a mass lesion in the lower lobe of the right lung. There was no family history of renal or other genitourinary cancers. The patient, with a 30-pack/year smoking history, was diagnosed with limited-stage SCLC on biopsy in October 2021. The patient was treated with four cycles of cisplatin + etoposide, and concurrent radiation therapy: 150 cGy fractions given twice daily for 30 fractions over 3 weeks, administered during cycle 1 of chemotherapy (total dose: 4500 cGy). After treatment for limited-stage small-cell lung cancer, significant regression was detected in 18-fluorine-fluorodeoxyglucose positron emission tomography/computed tomography (FDG PET/CT), and the patient continued oncology follow-up. The patient did not receive prophylactic cranial irradiation.

Twelve months after treatment, only an 11 mm lesion was detected under the skin of the right thigh on PET/CT, without any other metastatic foci, and was excised. The pathology report following excision revealed SCLC metastasis. In addition, a 5 mm metastatic left frontal lesion was detected on brain magnetic resonance imaging (MRI). This lesion was treated with stereotactic radiosurgery. The patient with radiologic and pathologic extensive stage SCLC was treated with six cycles of carboplatin, etoposide, and atezolizumab in January 2023. The patient's treatment was resumed with maintenance atezolizumab after July 2023. No primary SCLC or metastatic lesion was detected on follow-up imaging for approximately 1.5 years

Cite this article as: Özgür G, Kars M, Ceran İH, et al. Kidney metastasis of small cell lung cancer under immunotherapy. Bull Urooncol. 2026;25(1):27-30.

Address for Correspondence: Günal Özgür, MD, Marmara University Pendik Training and Research Hospital, Department of Urology, İstanbul, Türkiye
E-mail: gunalozgur91@hotmail.com **ORCID:** orcid.org/0000-0002-3847-0089
Received: 28.02.2025 **Accepted:** 24.06.2025 **Publication Date:** 18.03.2026

under maintenance atezolizumab therapy. However, on follow-up, FDG PET/CT detected a 44x40 mm lesion (SUV_{max}=13.6) in the anterior lower pole of the left kidney, which was classified as T1b according to the tumor-node-metastasis staging system (Figure 1). At the time of renal mass evaluation, the patient's serum creatinine was 1.43 mg/dL; eGFR was 40 mL/min/1.73 m^2; C-reactive protein was 3.84 mg/L; white blood cell count was 6.06×10^9/L; hemoglobin was 12.3 g/dL; and platelet count was 298×10^9/L. Liver function tests and electrolytes were within normal limits. Her body mass index was 31.3 kg/m^2 (height: 160 cm, weight: 80 kg), and Eastern Cooperative Oncology Group Performance Status performance status was 1. Due to decreased renal function and the associated risk of contrast-induced nephropathy, contrast-enhanced MRI was performed instead of triphasic CT. The patient who also underwent MRI was discussed in the uro-oncology board. The tumor was considered a second primary renal tumor by the uro-oncology board. Surgical treatment was recommended, and due to its location and apparent attachment to the proximal ureter and renal pelvis on imaging, nephrectomy was likely considered necessary. During laparoscopy, partial nephrectomy was considered; however, due to the tumor's infiltrative nature and ureteral involvement, radical nephrectomy was performed to preserve oncological principles. Pathology of the 5.6 cm diameter renal mass was determined to be SCLC metastasis (Figure 2). Pathology showed that tumor cells invaded renal parenchyma, perirenal adipose tissue, and renal sinus. The patient had no residual lesions after nephrectomy, and her treatment was continued with atezolizumab based on the council's decision.

Written informed consent was obtained from the patient for publication of this case report and any accompanying images.

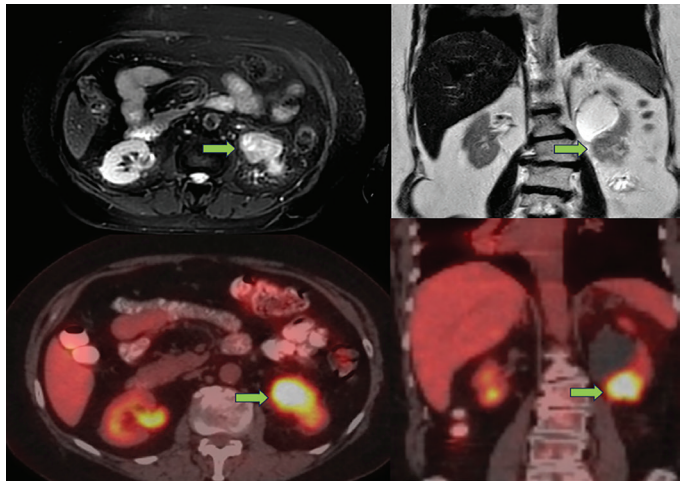

Figure 1. FDG PET/CT and MRI images of a kidney mass MRI (upper line) and FDG PET/CT (lower line) images of the kidney mass are shown. The green arrow indicates the kidney mass. MRI shows a lesion approximately 4 cm in size in the lower pole of the kidney. This lesion uptakes FDG (SUV_{max}=13.6)

FDG PET/CT: 18-fluorine-fluorodeoxyglucose positron emission tomography/computed tomography, MRI: magnetic resonance imaging

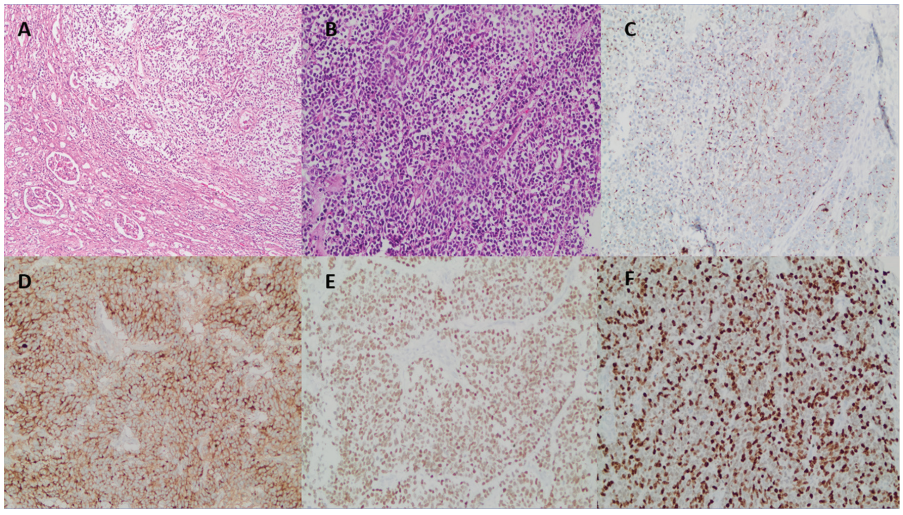

Figure 2. Histopathologic images of renal metastasis of small cell lung cancer

Microscopic examination revealed neoplastic cells with variable morphology, appearing round-to-oval in some areas and more spindle-shaped in others. These cells exhibited scant cytoplasm, hyperchromatic nuclei, granular chromatin, and an absence of prominent nucleoli. Features such as nuclear molding and crush artifacts were observed, along with a high mitotic index. Extensive areas of necrosis were present around the neoplastic cell clusters. Immunohistochemical studies demonstrated that the neoplastic cells were positive for PanCK, chromogranin, synaptophysin, and TTF-1. No immunoreactivity was observed with PAX-8. The Ki-67 proliferation index was approximately 70%.

A. Normal renal parenchyma is observed on the left side, while neoplastic cell infiltration is noted in the upper right area (hematoxylin and eosin, 100X).

B. Tumour cells have scant cytoplasm, poorly defined cell borders, and finely granular nuclear chromatin (hematoxylin and eosin, 200X).

C. A rim-and-dot pattern of PANCK expression is observed in the neoplastic cells (X200).

D. Diffuse synaptophysin expression is observed in the neoplastic cells (X200).

E. TTF-1 expression is observed in the tumor cells (X200).

F. Ki-67 proliferation index of approximately 70% is observed (X200).

PanCK: Pan-cytokeratin, TTF-1: Thyroid transcription factor-1, PAX: Paired box gene

Discussion

Renal metastasis of cancers is typically observed as solitary lesions (77.5%) (2,4). In patients with solitary lesions in the kidney, it is difficult to distinguish between metastases and primary renal tumors. SCLC metastasis can occur in all organs. However, renal metastasis of SCLC is very rare and difficult to differentiate from primary renal cell carcinoma (RCC) without histopathology (5). Imaging modalities such as ultrasonography, CT, MRI, and PET are frequently used for lung and kidney tumors. Unfortunately, there is no pathognomonic finding to determine whether the mass is a primary renal tumor or lung metastasis in a patient with a renal mass (1).

Although imaging cannot definitively distinguish between primary RCC and renal metastasis, some features may provide clues. According to previous reports, primary RCCs are generally larger, exophytic, and heterogeneous on contrast imaging, whereas renal metastases tend to be smaller, endophytic, and homogeneous (6,7). Moreover, primary RCCs are generally solitary, while metastases are more likely to be bilateral or multifocal. In our case, the lesion also appeared solitary.

Percutaneous renal biopsy can reveal the histology of radiologically indeterminate renal masses and may be useful in differentiating between primary RCC and metastases. It is particularly useful in patients with a known history of malignancy and in determining the most appropriate systemic or surgical treatment strategy (8).

As in our patient, these solitary renal tumors may usually be considered secondary cancer, and treated surgically as primary renal tumors. Lung cancer patients with renal spread usually have concomitant liver, bone and adrenal gland metastases (3). However, our patient had bone and brain metastases and had been followed up without progression for about 1.5 years under maintenance atezolizumab treatment. Therefore, suspicion of renal metastasis should be considered when a renal mass is detected in patients with SCLC and previous multiple metastases.

Guidelines on the treatment of renal metastasis need to be clearer. Surgical treatment positively impacts survival in selected patients with lung cancer (2). Especially in unilateral isolated cases, when the primary tumor is controlled, nephrectomy may be an appropriate approach (3,9). A multidisciplinary approach is necessary to ensure proper treatment in these patients.

The impact of immunotherapy on the localization of metastases in SCLC remains unclear. Given the rarity of renal metastases, there are no definitive data regarding the specific effects of immunotherapy on renal involvement. A study discussing the challenges in predicting immunotherapy responses emphasized that, despite its established role in SCLC treatment, variability in therapeutic outcomes—particularly across different metastatic sites—highlights the need for biomarkers to predict efficacy (10).

Immunotherapy may suppress microscopic metastases by enhancing systemic antitumor immunity. However, at the molecular level, its effectiveness may be limited in organs with low immune cell infiltration, such as the kidney. Experimental models and translational studies are required to better understand how immunotherapy influences metastatic tropism. Literature suggests that the location of metastases can affect treatment outcomes. In a study involving patients with metastatic RCC (mRCC), those with lung-only metastases had better survival rates compared to those with liver or bone metastases. Although this study focused on mRCC, it supports the idea that organ-specific tumor microenvironments and immune infiltration may modulate the efficacy of immunotherapy. Further research is warranted to investigate how immunotherapy influences metastasis in uncommon sites such as the kidneys (11).

Renal metastasis of SCLC is very rare. Most patients are asymptomatic and are diagnosed incidentally by imaging methods. Since imaging alone cannot reliably distinguish between primary and secondary renal tumors, histopathological confirmation remains essential for accurate diagnosis. In unilateral isolated renal metastasis, nephrectomy is an appropriate approach when the primary tumor is under control. A multidisciplinary approach is crucial to ensure appropriate management policy for these unusual cases. Furthermore, as immunotherapy becomes more widely used in SCLC, further research is needed to clarify its role in shaping atypical metastatic patterns, including renal involvement.

Ethics

Informed Consent: Written informed consent was obtained from the patient for publication of this case report and any accompanying images.

Acknowledgements

Publication: The results of the study were not published in full or in part in form of abstracts.

Contribution: There is not any contributors who may not be listed as authors.

Footnotes

Authorship Contributions

Surgical and Medical Practies: G.Ö., M.K., Y.Ş., Concept: G.Ö., M.K., Design: G.Ö., M.K., Y.Ş., Data Collection or Processing: G.Ö., İ.T.C., M.H.T., Y.Ş., Analysis or Interpretation: G.Ö., Literature Search: G.Ö., M.K., A.Ç., Writing: G.Ö., İ.T.C., M.H.T., A.Ç., Y.Ş.

Conflict of Interest: No conflict of interest was declared by the authors.

Financial Disclosure: The authors declared that this study received no financial support.

References

1. Bailey JE, Roubidoux MA, Dunnick NR. Secondary renal neoplasms. Abdom Imaging. 1998;23:266-274.
2. Zhou C, Urbauer DL, Fellman BM, et al. Metastases to the kidney: a comprehensive analysis of 151 patients from a tertiary referral centre. BJU Int. 2016;117:775-782.
3. Cazacu SM, SĂndulescu LD, Mitroi G, et al. Metastases to the kidney: a case report and review of the literature. Curr Health Sci J. 2020;46:80-89.

4. Becker WE, Schellhammer PF. Renal metastases from carcinoma of the lung. Br J Urol. 1986;58:494-498.
5. Lee JY, Kim J. Renal metastasis of small cell lung cancer with urothelial carcinoma of the bladder misdiagnosed as renal cell carcinoma. J Med Cases. 2019;10:253-256.
6. Karaosmanoglu AD, Onur MR, Karcaaltincaba M, et al. Secondary tumors of the urinary system: an imaging conundrum. Korean J Radiol. 2018;19:742-751.
7. Low G, Huang G, Fu W, et al. Review of renal cell carcinoma and its common subtypes in radiology. World J Radiol. 2016;8:484-500.
8. Ljungberg B, Albiges L, Bedke J, et al. Renal scell carcinoma. In: EAU Guidelines. Presented at the EAU Annual Congress, Paris 2024. Arnhem (The Netherlands): EAU Guidelines Office; 2024.
9. Adamy A, Von Bodman C, Ghoneim T, et al. Solitary, isolated metastatic disease to the kidney: Memorial Sloan-Kettering Cancer Center experience. BJU Int. 2011;108:338-342.
10. Tucker MD, Rini BI. Predicting response to immunotherapy in metastatic renal cell carcinoma. Cancers (Basel). 2020;12:3662.
11. Baston C, Parosanu AI, Stanciu IM, Nitipir C. Metastatic kidney cancer: does the location of the metastases matter? Moving towards personalized therapy for metastatic renal cell carcinoma. Biomedicines. 2024;12:1111.